Multiscale Methods for Wave Propagation Problems

HENRIK HOLST

Doctoral Thesis
Stockholm, Sweden 2011

Akademisk avhandling som med tillstånd av Kungl Tekniska högskolan framlägges
till offentlig granskning för avläggande av teknologi doktor i ämnet numerisk analys
fredagen den nionde december 2011 klockan 10:00 i E3, KTH Campus, Lindstedts-
vägen 3, Stockholm.

Abstract

Simulations of wave propagation in heterogeneous media and at high frequencies are important in many applications such as seismic-, electromagnetic-, acoustic-, fluid flow problems and others. These are classical multiscale problems and often too computationally expensive for direct numerical simulation. The smallest scales must be well resolved over a computational domain represented by the largest scale and this results in a very high computational cost. We develop and analyze numerical techniques based on the heterogeneous multiscale method (HMM) framework for such wave equations with highly oscillatory solutions u^ε where ε represents the size of the smallest scale. In these techniques the oscillatory microscale is approximated on small local microproblems of size ε in spatial and time directions. The solution of the microproblems are then coupled to a global macroscale model in divergence form $u_{tt} = \nabla \cdot F$ where the flux F is obtained from the microproblems. The oscillations can either originate from fluctuations in the velocity coefficients or from high frequency initial and boundary conditions. We have developed algorithms that couple micro and macroscales for both these cases. The choice of macroscale variables is inspired by the analytic theories of homogenization and geometrical optics respectively. In the first case local averages $u \approx u^\varepsilon$ are used on the macroscale. In the second case, phase ϕ and energy are natural macroscopic variables. There are two major goals of this research. One goal is to develop and analyze algorithms for simulating multiscale wave propagation with low computational complexity, and even independent of ε for finite time problems. This is seen in many examples in one, two and three dimensions. The other goal is to use wave propagation as a model to better understand the HMM framework. An example in this direction is simulation with oscillatory wave field over long time. The dispersive effects that then occur is well approximated by a HMM method that was originally formulated for finite time where added accuracy is required but no explicit adjustment to include dispersion, an evidence of the robustness of the method.

Sammanfattning

Simulering av högfrekventa vågor i heterogena material är viktigt i många tillämpningar, till exempel seismologi, elektromagnetism, akustik och strömningsmekanik. Dessa tillämpningar är exempel på klassiska multiskalproblem och har typiskt en för hög beräkningskostnad, i form av datortid och minne, för en direkt numerisk simulering. De minsta skalorna i problemet måste vara upplösta över ett område som representeras av dom största skalorna och detta innebär en hög beräkningskostnad. Vi har utvecklat och analyserat numeriska metoder för vågekvationer med snabbt oscillerande lösningar u^ε där ε representerar storleken på den minsta skalan. Metoderna är baserade på ramverket *heterogena multiskalmetoden* (HMM). I dessa metoder approximeras den hastigt oscillerande mikroskalan med små lokala mikroproblem av storleksordning ε i tids- och rumsriktning. Lösningen till mikroproblemen är kopplade till en global modell på makroskalan i divergensform $u_{tt} = \nabla \cdot F$, där flödet F ges av mikroproblemen. De hastiga oscillationerna kan härröras från snabba variationer i hastighetsfältet, begynnelsevillkor eller randvillkor. Vi har utvecklat algoritmer som kopplar mikro- och makroskalor i bägge fallen. Valet av makroskalvariabler inspireras av de analytiska metoderna homogenisering och geometrisk optik. I det första fallet används lokala medelvärden $u \approx u^\varepsilon$ på makroskalnivån. I det andra fallet är fas ϕ och energi bra val av makroskalvariabler. Det finns två huvudmål med vår forskning. Ett mål är att utveckla och analysera algoritmer för simulering av vågproblem med multipla skalor med låg beräkningskostnad (om möjligt, oberoende av ε) för problem över begränsad tid. Vi visar numeriska resultat från multiskalproblem i en, två och tre dimensioner. Det andra målet är att att använda vågutbredning som en modell för att bättre förstå HMM ramverket. Ett exempel på detta är simulering med oscillerande hastighetsfält över lång tid. Efter lång tid så uppträder dispersion. Vi har demonstrerat att vår HMM-metod, som ursprungligen var formulerad för begränsad tid, även kan appliceras på detta fall. För att få den rätta dispersionen krävs högre noggrannhetsordning, men metoden ändrar inte form. Detta visar på metodens robusthet.

Dedicated to
Laura

Preface

The thesis contains an introduction, one short abstract, four full length papers and a technical report containing relevant algorithms and computer codes.

Paper I (short)   Multiscale methods for the wave equation, *Sixth International Congress on Industrial Applied Mathematics (ICIAM07) and GAMM Annual Meeting*, volume 7. Wiley, 2007. [21]

This paper is the first publication of the research and is included for completeness. The content is largely covered by Paper II.

Paper II   Multiscale Methods for the Wave Equation, *Comm. Math. Sci.*, 9(1):33–56, Mar 2011. [24]

Paper III   Multiscale Methods for Wave Propagation in Heterogeneous Media Over Long Time, *Numerical Analysis and Multiscale Computations*, volume 82 of *Lect. Notes Comput. Sci. Eng.*, pages 167–186. Springer Verlag, 2011. [25]

Paper IV   Analysis of HMM for One Dimensional Wave Propagation Problems Over Long Time, *arXiv:1111.2541*. [22]

Paper V   Multiscale Methods for One Dimensional Wave Propagation with High Frequency Initial Data, TRITA-NA 2011:7. [23]

Paper VI   Algorithms and Codes for Wave Propagation Problems, TRITA-NA 2011:6. [34]

Most of the papers are co-authored with my supervisors Björn Engquist and Olof Runborg. The distribution of the contributions to the papers is typical for the student - supervisor situation. Many suggestions, part of the analysis and a number of corrections where done by the supervisors. I did most of the analytical parts, all of the numerical simulations and almost all of the writing.

Acknowledgements

Contents

Part I

Introductory Chapters

Chapter 1

Goals

The main goal in this thesis is to better understand a new class of multiscale methods developed for high frequency wave propagation. Multiscale wave propagation problems are of both theoretical and practical importance. Many applications relating to wave propagation is multiscale by nature, and arises in areas from seismic problems, electromagnetic waves, acoustics, and fluid flow- problems. The methods are developed within the framework of heterogeneous multiscale methods (HMM). One of our two main goals has been to give the multiscale and wave community a better understanding of the problems and what challenges remains to be solved for reliable and efficient numerical methods for multiscale wave propagation problems. The second goal has been to illustrate new multiscale methods based on the HMM framework. We have been interested in the development, analysis and testing of these methods. Hopefully we can give some inspiration to others to develop more complicated HMM methods based on key ideas suggested here: how to choose macroscopic variables, setup a micro problem, and how to describe the interchange between micro and macro variables. But not only that, but also how to address intricate questions such as consistency between macro and micro scales. We will see how this is a key factor in the HMM method for wave propagation over long time.

Part I of this thesis is organized as follows: First is a discussion on wave propagation problems without any special considerations about scales or how to reduce computational effort. This is followed by a discussion on multiscale problems from a general perspective and a discussion about multiscale wave propagation problems where I and my co-authors make an argument for our contribution to this field. Thereafter, we give a summary of our papers on this subject. Papers I & II considers multiscale waves traveling in a highly oscillatory media for a finite time whereas papers III & IV discuss how our method can be tuned to resolve multiscale waves traveling long distances for long time. In this case dispersive effects must be taken into account. In Chapter 5 we give a summary of paper V and our work for high frequency waves. In this regime the material is smooth and our HMM method is

modeled from ideas in geometrical optics. In Chapter 6 we discuss ideas that can be added to the work we have done on the subject of numerical methods for multiscale wave propagation. Part II of this thesis contains the six included papers.

Chapter 2

Background

Waves are an important subject in physics. Many physical phenomena shows a wavelike behavior. The linear wave equation is a partial differential equation which is widely used in fields such as acoustics, elasticity and electromagnetism. The theory of the wave equation was first developed in these areas. The linear wave equation has shown great success as an approximation for compressible fluids in such cases when viscosity, heat conduction and nonlinearities are neglected. In this thesis we will consider the linear wave equation. The aim in this chapter is to give some background theory to the concepts related to linear and multiscale waves; methods for such problems; and three mathematical models for different regimes of multiscale wave propagation. We will also describe a concept of a certain type of local smoothing operators, which will be frequently used in our multiscale methods.

2.1 Waves

The linear partial differential equation,

$$u_{tt}(x,t) - \nabla \cdot (A(x)\nabla u(x,t)) = 0, \qquad \Omega \times \mathbb{R}, \tag{2.1}$$

with initial data,

$$u(x,0) = u_0(x), \quad u_t(x,0) = u_1(x), \qquad \forall x \in \Omega, \tag{2.2}$$

is a widely used mathematical model for wave propagation. The domain Ω is the entire $\mathbb{R}^d$ for a pure initial value problem or a subset of $\mathbb{R}^d$ for an initial boundary value problem. In the latter case, the typical boundary conditions for u are periodic, reflecting or non-reflecting. The solution $u(x,t)$ will describe the wave at position x in space t in time. The parameter A describes the local wave speed squared. As we said in the introduction, the wave equation is a good mathematical model for many wave like phenomena that occur in nature. It is used as one of the fundamental equations in acoustics, optics, seismology, electromagnetic waves, quantum-mechanics

and fluid dynamics. In each case u and A will describe the physical properties of the problem. The model (2.1) was first studied by Jean le Rond d'Alembert, Leonhard Euler, Daniel Bernoulli and Joseph Louis Lagrange. d'Alembert formulated the solution for this problem in one dimension when $A(x) = c^2$ is constant, in a particularly simple form,

$$u(x,t) = \frac{1}{2}\left(u_0(x - ct) + u_0(x + ct)\right) + \frac{1}{2c}\int_{x-ct}^{x+ct} u_1(s)\,\mathrm{d}s. \qquad (2.3)$$

The wave equation has several useful mathematical properties and we will list a few of the most important things we will use later:

Energy is preserved: solutions u preserves a quantity denoted as the energy of the solution,

$$E(x,t) = \frac{1}{2}|u_t(x,t)|^2 + \frac{|A(x)|}{2}|\nabla u(x,t)|^2, \qquad (2.4)$$

in the sense that

$$\int E(x,t)\,\mathrm{d}x = \int E(x,0)\,\mathrm{d}x, \qquad \forall t \in \mathbb{R}. \qquad (2.5)$$

This holds true if A decays fast enough as $|x| \to \infty$ or if we have a periodic problem where both u and A are periodic in x.

Linearity: The linearity of the wave equation implies, for two given solutions to (2.1) denoted $v_1(x,t)$ and $v_2(x,t)$, that any linear combination of v_1 and v_2 will also solve the wave equation, where the solution $u(x,t)$ is of the form,

$$u(x,t) = \alpha v_1(x,t) + \beta v_2(x,t), \qquad \alpha, \beta \in \mathbb{R}, \qquad (2.6)$$

with the initial data,

$$\begin{cases} u(x,0) = \alpha v_1(x,0) + \beta v_2(x,0), \\ u_t(x,0) = \alpha(\partial_t v_1)(x,0) + \beta(\partial_t v_2)(x,0), \end{cases} \qquad \forall x \in \Omega. \qquad (2.7)$$

Finite speed of propagation: Information travels with a finite speed in the wave equation. In the solution formula (2.3) the constant c is the speed of which information propagates. A crude estimate for the maximum speed $c_{\max}$ for a non-constant A is to take $c_{\max} = \sup \sqrt{|A(x)|}$. We will use this fact later to estimate the speed of waves arising from boundary conditions.

2.2   Numerical Multiscale Problems and Methods

When we seek to find a solution to a problem, we need a defined method to solve this problem. But to apply a general problem solving method we need the problem

statement to be well defined. Thus, we shall start our discussion by asking: What *is* a multiscale problem? A definition with only examples is not terrible useful so Weinan et. al. [17, 18] defined:

> A multiscale problem is a problem where one can make use of special features in the problem.

They continued and defined four types of multiscale problems:

Type A: Problems that contain isolated defects or singularities such as cracks, dislocations, shocks and contact lines. For these problems the microscopic models is only necessary near defects or singularities. Further away it is adequate to use the macroscopic models. The micro-macro coupling is localized.

Type B: Problems that require "first-principle-based" constitutive modeling. One example is the homogenization problem for elliptic equations of the type

$$- \nabla \cdot (A^\varepsilon \nabla U) = f. \tag{2.8}$$

Under fairly general conditions that amount to scale separation for the coefficient A^ε, it can be shown [7], that the effective macroscale model take the form,

$$- \nabla \cdot (\bar{A} \nabla U) = f, \tag{2.9}$$

where $\bar{A}$ is called the homogenized coefficient. We will return to this theory in Section 2.4. The HMM method for this problem would provide $\bar{A}$ from microscale simulations at a cost much lower than solving the entire problem with A^ε.

Type C: Problems with a mixed character between type A & type B problems.

Type D: Problems that exhibits self-similarity in scales. For instance problems in statistical physics, fractals or turbulent transport.

It is stressed that one can define more types of multiscale problems, than those examples above.

It is typically very computationally costly to solve multiscale problems by traditional numerical techniques. The smallest scale must be well represented over a domain, which is determined by the largest scales. For wave propagation the smaller scales may originate from high frequencies or from strong variations in the wave velocity field. We will focus on the latter case. Examples of such variable velocity problems are seismic wave propagation in subsurface domains with inhomogeneous material properties and microwave propagation in complex geometries.

A new class of numerical multiscale methods couples simulations on macro and micro scales [17, 37]. We are using the framework of the heterogeneous multiscale method (HMM) [17, 18, 16]. In HMM a numerical macro scale method gets

necessary information from micro scale models that are only solved on small sub-domains. This framework has been applied to a number of multiscale problems, for example, ODEs with multiple time scales [31], elliptic and parabolic equations with multiscale coefficients [19, 45, 1], kinetic schemes [18] and large scale MD simulation of gas dynamics [40]. Other potential applications of the specific HMM method we will develop are in seismic-, acoustic-, electromagnetic- or and other wave propagation problems in cluttered domains.

The Heterogeneous Multiscale Method

The heterogeneous multiscale method [17, 18] is a general framework for designing multiscale method and not *a method* itself. The name *heterogeneous* should emphasize that the models at different scales are allowed to be different as it often is in real world applications. The HMM framework provides a template for new methods for multiscale problems.

In the HMM framework, the general setting of a multiscale problem is the following: we assume that there exist two models, a micro model $f(u^\varepsilon, d^\varepsilon) = 0$ describing the full problem and a coarse macro model $F(U, D) = 0$. The micro model is accurate but is expensive to compute by traditional methods. The macro model gives a coarse scale or low frequency solution U, which is assumed to be a good approximation of the microscale solution u^ε and is less expensive to compute. The model is however incomplete in some sense and requires additional data. We assume that $F(U, D) = 0$ can still be discretized by a numerical method, called the macro solver. A key idea in the HMM method is to provide the missing data D in the macro model using a local solution to the micro model. The micro model solution u^ε is computed locally on a small domain with size proportional to the microscale. The initial data and boundary conditions, represented by d^ε, for this computation are constrained by the macroscale solution U.

The HMM framework consists of two main components:

1. Selection of a macroscopic equation and solver. In this step we ignore that that the model is incomplete in some sense and we discretize the macroscopic PDE as if all quantities where known.

2. Estimating missing macroscale data D using microscale model. This step contains the following components:

    (a) Constrained microscale simulation: Formulate $d = d(U)$ to obtain boundary and initial conditions to the microscopic problem. The operator which maps U into d^ε is called a *reconstruction operator* in the HMM terminology.

    (b) Data processing: Use the solution u^ε of the previous step to obtain $D = D(u^\varepsilon)$. The function that maps u^ε to D is called a *compression operator* in the HMM terminology.

2.3 Multiscale Waves

Suppose we have a wave equation formulated as an initial value problem,

$$\begin{cases} u_{tt}^{\varepsilon} - \nabla \cdot (A^{\varepsilon} \nabla u^{\varepsilon}) = 0, & \Omega \times [0, T^{\varepsilon}], \\ u^{\varepsilon}(x, 0) = u_0^{\varepsilon}(x), \quad u_t^{\varepsilon}(x, 0) = u_1^{\varepsilon}(x), & \forall x \in \Omega, \end{cases} \tag{2.10}$$

on a smooth domain $\Omega \subset \mathbb{R}^N$, $|\Omega| = \mathcal{O}(1)$ and generally with boundary conditions.

The mathematical model (2.10) used to describe a multiscale wave propagation problem has ε marked on almost all quantities. This is to indicate that this quantity can directly depend on ε in some way. We will focus on three different types of problems of this form:

a) Non-oscillatory initial data (u_0 and u_1); finite $T = \mathcal{O}(1)$; and a positive A^{ε}. We call this the homogenization regime. The mathematical multiscale model called homogenization is described in detail in Section 2.4.

b) Same as above but $T^{\varepsilon} \to \infty$ as $\varepsilon \to 0$. We will show in Section 2.5 that the mathematical model presented in the homogenization section is not sufficient to describe the dispersive character of the solution in the case when A^{ε} is oscillatory.

c) In the last case we take A and T without ε dependence. The initial data u_0^{ε} and u_1^{ε} depends on ε. We call this regime the high frequency regime. The effective models for this kind of multiscale wave propagation problem (high frequency problem) is described in Section 2.6.

We consider variations on these models in Section 6.

Computing the full solution to (2.10) with standard direct methods such as finite differences [32], finite elements [10], finite volume [39], discontinuous galerkin [14] or by spectral methods [11, 54] is costly. They are all computational costly to use because the smallest scales must be resolved over a much lager domain Ω. Instead of trying to obtain a complete solution we will create a HMM process which has a reduced computational complexity and gives a coarse scale solution without a full resolution of the high frequency scales proportional to ε. However, this coarse scale solution incorporates fine scale effects.

Our Contribution

The goal of our research is to better understand the HMM process using the example of wave propagation and also to derive computational techniques for future practical wave equation applications. We hope that our work can lead to efficient and practically methods for multiscale wave propagation problems.

One contribution is a convergence proof in the multidimensional case that includes a discussion on computational complexity. The analysis is partially based on the mathematical homogenization theory, [7, 13]. This theory gives the macro scale

limit equations as $\varepsilon \to 0$. The numerical methods apply to a more general class of problems for which the explicit form of the homogenized equation may not be known. A central contribution is the development and testing of numerical HMM techniques in one, two and three space dimensions. Our second contribution is the exploration of HMM methods for simulation of multiscale wave propagation over long time. The effective equation for long time is different from the finite time homogenized equation. Dispersive effects enter, and the effective equation must be modified [49]. It is interesting to notice that our HMM approach with just minor modifications accurately captures these dispersive phenomena.

The third major contribution is a new multiscale method for high frequency waves. The new method gives comparable results to geometrical optics (GO) [28] when a is smooth but our method is more general than GO. Our HMM method gives the correct reflected and transmitted energy in the case when a has a jump on the microscale. The HMM method formulates a coupled system for left and right going energy $E_t + F_x = 0$ where the flux F is computed from either the material a when a is smooth, or by solving a microproblem where GO fails. Our methods bears some resemblance to the transfer-matrix method, which is used in optics and acoustics to analyze the propagation of electromagnetic or acoustic waves through a stratified (layered) medium [9].

2.4   Homogenization of the Wave Equation

The goal of classical homogenization is finding limiting equations and solutions to a wide range of problems with a suitable "scale", denoted here by ε, which is allowed to pass to zero in the limit. In the setting of composite materials, consisting of two or more mixed constituents, homogenization theory gives the macroscopic properties of the composite. The macroscopic properties are often different than the average of the individual constituents that makes up the composite [13]. When the scale in the micro structure ε goes to zero, the homogenized equations and the homogenized solution can be used as an approximation of the full equation typically with an accuracy of order $\mathcal{O}(\varepsilon)$. Homogenization is a good idea also from a numerical perspective. The homogenized equation is often easier to solve numerically than the full equation which might have fast oscillations depending on the microscale composition.

The homogenized wave equation in d-dimensions can in certain cases be computed analytical by replacing u^ε in the PDE with a multiscale expansion on the form

$$u^\varepsilon(x) = u^0(x, y) + \varepsilon u^1(x, y) + \varepsilon^2 u^2(x, y) + \cdots \quad \text{where} \quad y = \frac{x}{\varepsilon} \qquad (2.11)$$

and where all functions are Y-periodic, $Y = [0, 1]^d$, in their y argument. By plugging the series (2.11) into (2.10) and collecting equal powers of ε we can form a system of equations for $u^0, u^1, \ldots$ The solution u^0 is what we call the homogenized

solution in the cases where the formal multiscale expansion agrees with strict homogenization theory. It can be shown that $u^0(x, y) = u^0(x)$ and u^0 does not depend on ε. We also often denote $u^0(x)$ by $\bar{u}(x)$. This method gives the correct solution in most cases but not always. Also the multiple-scale series method does not directly provide a rigorous proof since there is nothing a priori that says that the right hand side of (2.11) converges to u^ε. Other homogenization techniques that generalizes classical homogenization include 2-scale convergence, Γ-convergence and G-convergence. We refer to [46, 43, 3, 13, 35, 47, 41, 30, 44] for further details about these other techniques.

We consider the multiscale wave equation (2.10) in d-dimensions, formulated as an initial value problem. We assume that $A^\varepsilon(x) = A(x, x/\varepsilon)$ where A is, symmetric, positive definite and locally Y-periodic. By locally Y-periodic we mean that $A(x, y)$ is periodic with respect to $y \in Y$ if x is held fixed. A classic result [7], shows that the solution to the equation (2.12) will converge to the solution of the homogenized wave equation,

$$\begin{cases} u_{tt} - \nabla \cdot (\bar{A} \nabla u) = 0, & \Omega \times [0, T], \\ u(x, 0) = u_0(x), \quad u_t(x, 0) = u_1(x), & \forall x \in \Omega, \end{cases} \tag{2.12}$$

as $\varepsilon \to 0$ and for fixed T. We assume the variation in the initial data u_0 and u_1 is comparable to the slow scale, but this is not a necessary condition as we show in Section 2.4. The matrix $\bar{A}$ is independent of ε, symmetric, positive definite and the elements can be computed with explicit formulas. In the one-dimensional case, the matrix $\bar{A}$ is equal to the harmonic average of A^ε over one cell Y,

$$\bar{A}(x) = \left(\int_0^1 \frac{\mathrm{d}y}{A(x, y)} \right)^{-1}. \tag{2.13}$$

In a d-dimensional setting $\bar{A}$ is given implicitly by the relations [13, Proposition 6.8],

$$\bar{A}_{ij} = \int_Y \nabla \hat{w}_{e_i} \cdot A \nabla \hat{w}_{e_j} \, \mathrm{d}y, \qquad 1 \le i, j, \le N, \tag{2.14}$$

where $\hat{w}_\lambda$ $(1 \le \lambda \le d)$ is defined as

$$\hat{w}_\lambda := -\hat{\chi}_\lambda + \lambda \cdot y, \tag{2.15}$$

and χ_λ $(1 \le \lambda \le d)$ are the unique solutions to the cell problem,

$$\begin{cases} -\nabla \cdot (A(y) \nabla \hat{\chi}_y) = -\nabla \cdot (A\lambda), & \text{on } Y, \\ \int_Y \hat{\chi}_\lambda = 0, \quad \hat{\chi}_\lambda \quad Y\text{-periodic}. \end{cases} \tag{2.16}$$

In a typical situation A is not precisely periodic, so the theory above does not apply. Still there might exist an equation of the form (2.12) which gives a smooth solution u, with no ε-scale, that is a good approximation of u^ε. However, there may not be a known expression for $\bar{A}$ in that case. This will be the foundation for our HMM method we will describe later on.

Classical Theorem: Homogenization of the Wave Equation

Let us show a typical rigorous result about homogenization of the wave equation. Suppose the wave equation is given on the form

$$\begin{cases} u_{tt}^\varepsilon - \nabla \cdot (A^\varepsilon \nabla u) = h^\varepsilon & \Omega \times [0,T], \\ u^\varepsilon = 0 & \partial\Omega \times [0,T], \\ u^\varepsilon(x,0) = u_0^\varepsilon(x) & \forall x \in \Omega, \\ u_t^\varepsilon(x,0) = u_1^\varepsilon(x) & \forall x \in \Omega. \end{cases} \tag{2.17}$$

Here $A^\varepsilon(x) = A(x/\varepsilon)$ where $A \in L^\infty(\Omega)^{N \times N}$ is symmetric, Y-periodic, bounded and positive definite uniformly in x, i.e., there exists constants $c > 0$ and $d > 0$ independent of x such that

$$\begin{aligned} \lambda^T A^\varepsilon(x)\lambda &\geq c\|\lambda\|^2 & \forall \lambda \in \mathbb{R}^N, \\ \|A^\varepsilon(x)\lambda\| &\leq d\|\lambda\| & \forall \lambda \in \mathbb{R}^N. \end{aligned} \tag{2.18}$$

We consider solutions to a variational form of (2.17)

$$\begin{cases} \text{Find } u^\varepsilon \in \mathcal{W}_2 \text{ such that} \\[2mm] \langle u_{tt}^\varepsilon, v \rangle_{H^{-1}(\Omega), H_0^1(\Omega)} + \displaystyle\int_\Omega A^\varepsilon(x)\nabla u_\varepsilon(x,t)\nabla v(x)\,\mathrm{d}x \\[2mm] \qquad = \displaystyle\int_\Omega h^\varepsilon(x,t)v(x)\,\mathrm{d}x \qquad \mathcal{D}'(0,T), \quad \forall v \in H_0^1(\Omega) \\[2mm] u^\varepsilon(x,0) = u_0^\varepsilon(x) \qquad \forall x \in \Omega, \\[1mm] u_t^\varepsilon(x,0) = u_1^\varepsilon(x) \qquad \forall x \in \Omega. \end{cases} \tag{2.19}$$

where

$$\mathcal{W}_2 = \left\{ v : v \in L^2(0,T; H_0^1(\Omega)), v' \in L^2(\Omega \times [0,T]) \right\}. \tag{2.20}$$

Then one can show the following theorem. The proof is classical and can be found in [13] and [7].

Theorem 1. *Suppose that $h^\varepsilon \in L^2(\Omega \times [0,T])$, $u_0^\varepsilon \in H_0^1(\Omega)$, and $u_1^\varepsilon \in L^2(\Omega)$. Let u^ε be the solution of (2.19) with A^ε defined as above. Assume that*

$$\begin{cases} i) & u_0^\varepsilon \rightharpoonup u_0 & \text{weakly in } H_0^1(\Omega) \\ ii) & u_1^\varepsilon \rightharpoonup u_1 & \text{weakly in } L^2(\Omega) \\ iii) & h^\varepsilon \rightharpoonup h & \text{weakly in } L^2(\Omega \times [0,T]). \end{cases} \tag{2.21}$$

Then, one has the convergences (in the topology of pointwise convergence),

$$\begin{cases} i) & u^\varepsilon \rightharpoonup \bar{u} & \text{weakly* in } L^\infty(0,T; H_0^1(\Omega)) \\ ii) & u_t^\varepsilon \rightharpoonup \bar{u}_t & \text{weakly* in } L^\infty(0,T; L^2(\Omega)) \\ iii) & A^\varepsilon \nabla u^\varepsilon \rightharpoonup \bar{A}\nabla\bar{u} & \text{weakly in } L^2(\Omega \times [0,T])^N. \end{cases} \tag{2.22}$$

where $\bar{u}$ is the solution of the homogenized problem:

$$\begin{cases} \bar{u}_{tt} - \nabla \cdot (\bar{A}\nabla u) = h & \Omega \times [0,T], \\ \bar{u} = 0 & \partial\Omega \times [0,T], \\ \bar{u}(x,0) = u_0(x) & \forall x \in \Omega, \\ \bar{u}_t(x,0) = u_1(x) & \forall x \in \Omega, \end{cases} \tag{2.23}$$

and $\bar{A}$ is constant, symmetric, positive definite and given by (2.14), (2.15) and (2.16).

2.5 Effective Equation for Long Time Wave Propagation

In this section we will describe a theory for appreciative solutions to the long time wave equation,

$$\begin{cases} u_{tt}^\varepsilon - \nabla \cdot (A^\varepsilon \nabla u^\varepsilon) = 0, & \Omega \times [0, T^\varepsilon], \\ u^\varepsilon(x,0) = u_0(x), \quad u_t^\varepsilon(x,0) = u_1(x), & \forall x \in \Omega, \end{cases} \tag{2.24}$$

where $T = \mathcal{O}(\varepsilon^{-2})$ and Ω-periodic boundary conditions on u^ε.

In the classical homogenization theory for the wave equation the homogenized solution $\bar{u}$ satisfies a homogenized PDE (2.12). The solution $\bar{u}$ is a good approximation to the exact solution u^ε such that $\|u^\varepsilon(t,\cdot) - \bar{u}(t,\cdot)\|_{L^2} = \mathcal{O}(\varepsilon)$, up to a fixed time T independent of ε. In the long time equation (2.24), the homogenized solution is not able to describe the dispersion that might occur in the exact solution u^ε due to the fast oscillations in A^ε. Here the term dispersion refers to frequency-dependent effects in the wave propagation.

Let us illustrate the dispersive effects by an example. We consider a one-dimensional example where we solved (2.24) with $\varepsilon = 0.01$ and

$$\begin{cases} A^\varepsilon(x) = A(x/\varepsilon), \quad A(y) = 1.1 + \sin 2\pi y, \\ u(x,0) = \exp(-100x^2) + \exp(-100(1-x)^2), \quad u_t(x,0) = 0, \end{cases} \tag{2.25}$$

over $\Omega = [0,1]$ with periodic boundary conditions. The corresponding homogenized equation, valid up to $T = \mathcal{O}(1)$, will have $\bar{A} = \sqrt{0.2\bar{1}}$. Since we have periodic boundary conditions, the solution to the corresponding homogenized equation will be periodic in time with period $1/\sqrt{\bar{A}} \approx 1.47722$. We will compute the solution to (2.25) for 1, 10 and 100 periods. We see in Figure 2.1 that after 100 periods there is an $\mathcal{O}(1)$ error between the true solution u^ε and the homogenized solution $\bar{u}$ which thus fails to capture the dispersive behavior of the solution after long time. In [49], Santosa and Symes derived an equation for which approximates u^ε which have a L^2 error of order $\mathcal{O}(\varepsilon) + \mathcal{O}(\varepsilon^3 t)$. We call their equation the effective equation for long time wave propagation. Their theory extends the effective model (2.12) with
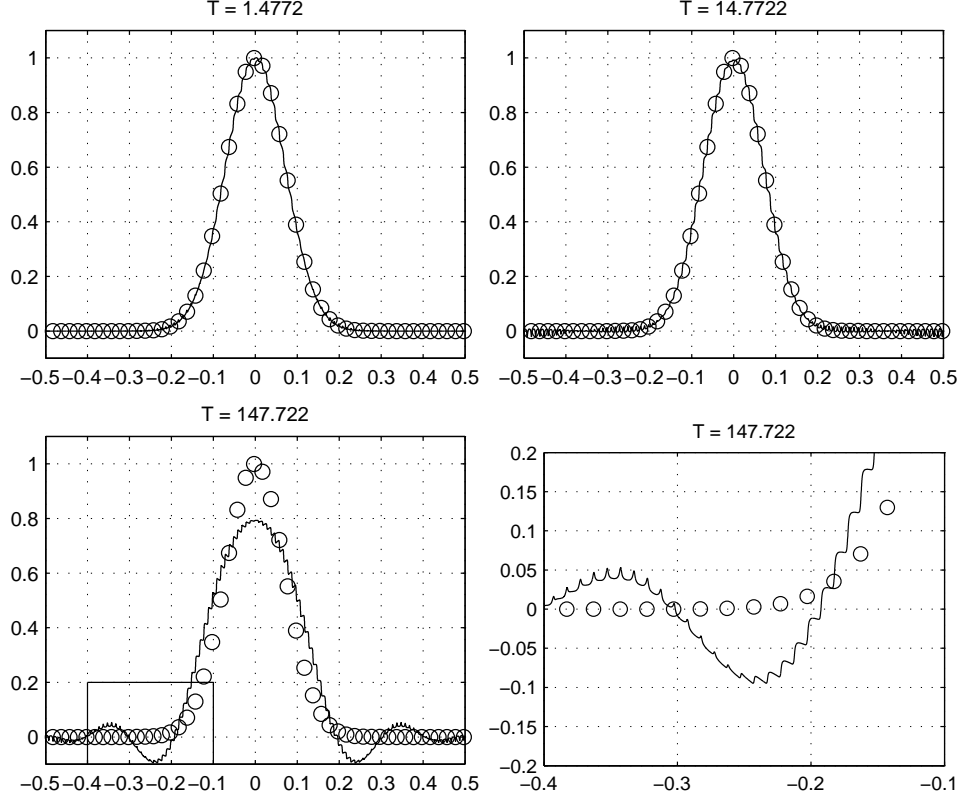
Figure 2.1: Finite difference computation of (2.25) at $T = 1.47722$, $T = 14.7722$ and $T = 147.722$ (1, 10 and 100 periods of the homogenized solution) and the corresponding homogenized solution (circles). As we can see the homogenized solution does not capture the dispersive effects that occur.

additional terms, from $T = \mathcal{O}(1)$ up to time $T = \mathcal{O}(\varepsilon^{-2})$. In one dimension for $A^{\varepsilon}(x) = A(x/\varepsilon)$ and $A(y)$ is 1-periodic, the effective equation has the form,

$$
\begin{cases}
u_{tt} - \bar{A}u_{xx} - \beta\varepsilon^2 u_{xxxx} = 0, & \Omega \times [0, T^{\varepsilon}], \\
u(x,0) = u_0(x), \quad u_t(x,0) = u_1(x), & \forall x \in \Omega,
\end{cases}
\tag{2.26}
$$

where $\bar{A}$ is the same $\bar{A}$ as in homogenization theory and β is a functional of A. Santosa and Symes provided a formula for β in their theory only when $A^{\varepsilon}(x) = A(x/\varepsilon)$, with no slow variations. In this case both β and $\bar{A}$ will be constant. They did not consider the case when $A^{\varepsilon}(x) = A(x, x/\varepsilon)$ has both slow and fast variations.

Analysis of the Effective Equation for Long Time Wave Propagation

In this section we will derive the expression for the effective equation (2.26) and also give a way to compute β from $A(y)$. In one dimension and for $A^\varepsilon(x) = A(x/\varepsilon)$ and A is 2π-periodic, Santosa and Symes gives the following expression for β,

$$\beta = \frac{\Omega_1 \Omega_3}{12\pi^2}, \qquad (2.27)$$

where the constants Ω_1 and Ω_3 are functions of the tensor A [49, (36, 37)]. The constants Ω_1 and Ω_3 are then computed from the expressions

$$
\begin{cases}
\Omega_1^2 = \bar{A}, \\
\dfrac{\Omega_3}{\pi^2} = \dfrac{3\Omega_1^3}{2\pi^3} \iiint_\Psi \dfrac{\mathrm{d}y\,\mathrm{d}s\,\mathrm{d}r}{A(r)} + \dfrac{3\Omega_1^5}{2\pi^3} \iiint_\Psi \dfrac{\mathrm{d}y\,\mathrm{d}s\,\mathrm{d}r}{A(y)A(r)} \\
\qquad - \bar{A}\left[\dfrac{1}{\Omega_1} + \dfrac{3\Omega_1}{\pi^2} \iint_{\Psi'} \dfrac{\mathrm{d}y\,\mathrm{d}r}{A(r)} - \dfrac{3\Omega_1^3}{4\pi^4} \left(\iint_{\Psi'} \dfrac{\mathrm{d}y\,\mathrm{d}r}{A(r)} \right)^2 \right], \\
\Psi = \{0 \le y \le 2\pi, 0 \le r \le y, 0 \le s \le r\}, \quad \Psi' = \{0 \le y \le 2\pi, 0 \le r \le y\}.
\end{cases}
\qquad (2.28)
$$

In [34] we provide a Maple code which computes the above integral given $A(x, y)$ where A is 2π-periodic in y.

We will now derive (2.26) and an expression for β. Let us first give some definitions: Let ω_m^2 and ψ_m be the eigenvalues and eigenfunctions of the shifted cell (eigenvalue) problem [7, pp. 614],

$$
\begin{cases}
-(\partial_y + ik)\,A(y)\,(\partial_y + ik)\,\psi(y, k) = \omega^2(k)\psi(y, k), & Y \times Y, \\
\psi(y, k) \text{ is } Y\text{-periodic in } y,
\end{cases}
\qquad (2.29)
$$

where $Y = [0, 1]^d$, $i = \sqrt{-1}$ and $k \in \mathbb{R}^d$. Let $v_m(x, k)$ be the scaled Bloch-waves,

$$v_m(x, k) = \psi_m(x/\varepsilon, \varepsilon k)\exp(ik \cdot x), \qquad (2.30)$$

which satisfies

$$-\partial_x\left(a\left(\frac{x}{\varepsilon}\right)\partial_x v_m\right) = \frac{1}{\varepsilon^2}\omega_m^2(\varepsilon k)v_m. \qquad (2.31)$$

The functions U_m and $\hat{f}_m$ are defined as the projection of u^ε and f on v_m,

$$U_m(k, t) = \int u^\varepsilon(x, t)v_m^*(x, k)\,\mathrm{d}x, \quad \hat{f}_m(k) = \int f(x)v_m^*(x, k)\,\mathrm{d}x. \qquad (2.32)$$

Throughout this section we assume that the initial data $f(x)$ is a band limited function. The following theorem from [49] then states that if we expand the solution to the wave equation in the basis given by $\{v_m\}$, the terms with $m \ge 1$ are bounded by $\mathcal{O}(\varepsilon)$ in L^2 uniformly in time.

Theorem 2 (Santosa & Symes). *Suppose u^ε solves (2.24) with $u_1(x) = 0$ and expand*

$$u^\varepsilon(x,t) = \int_{Y/\varepsilon} U_0(k,t)v_0(x,k)\,\mathrm{d}k + \sum_{m=1}^{\infty}\int_{Y/\varepsilon} U_m(k,t)v_m(x,k)\,\mathrm{d}k. \qquad (2.33)$$

Then

$$\int_{\mathbb{R}^3}\left|\sum_{m=1}^{\infty}\int_{Y/\varepsilon} U_m(k,t)v_m(x,k)\,\mathrm{d}k\right|^2\,\mathrm{d}x \le C\varepsilon^2. \qquad (2.34)$$

Here C is independent of ε and t but depends on the H^2-norm of the initial data f and the L^∞-norm of a and ∇a.

See [49] for a proof.

We denote the first term in (2.33) by u_0 and note that $\hat{f}_0(k)$ has compact support if $f(x)$ is band limited, see [49]. Then, for some fixed L,

$$u_0(x,t) = \frac{1}{2}\int_{Y/\varepsilon}\hat{f}_0(k)v_0(x,k)\exp(\pm i\omega_0(\varepsilon k)t/\varepsilon)\,\mathrm{d}k \qquad (2.35)$$

$$= \frac{1}{2}\int_{-L}^{L}\hat{f}_0(k)\psi_0(x/\varepsilon,\varepsilon k)\exp(ikx + i\omega_0(\varepsilon k)t/\varepsilon)\,\mathrm{d}k. \qquad (2.36)$$

We now Taylor expand ψ_0 in the second argument and use the fact that $\psi_0(x,0) \equiv 1$. This gives

$$u_0(x,t) = \frac{1}{2}\int_{-L}^{L}\hat{f}_0(k)(\psi_0(x/\varepsilon,0) + \mathcal{O}(\varepsilon k))\exp(ikx + i\omega_0(\varepsilon k)t/\varepsilon)\,\mathrm{d}k \qquad (2.37)$$

$$= \frac{1}{2}\int_{-L}^{L}\hat{f}_0(k)\exp(ikx + i\omega_0(\varepsilon k)t/\varepsilon)\,\mathrm{d}k + \mathcal{O}(\varepsilon). \qquad (2.38)$$

Next we Taylor expand $\omega_0(\varepsilon k)$ around $k = 0$ and use that the facts that $\omega_0(0) = 0$ and that by symmetry all odd derivatives of $\omega_0^2(k)$ at $k = 0$ are zero,

$$\omega_0(\varepsilon k) = \omega_0(0) + \varepsilon k\omega_0'(0) + \frac{\varepsilon^2 k^2}{2!}\omega_0''(0) + \frac{\varepsilon^3 k^3}{3!}\omega_0^{(3)}(0) + \mathcal{O}(\varepsilon^4 k^4) \qquad (2.39)$$

$$=: \tilde{\omega}_0(\varepsilon k) + \mathcal{O}(\varepsilon^4 k^4), \qquad (2.40)$$

and plug this expansion into the expression for u_0,

$$u_0(x,t) = \frac{1}{2}\int_{-L}^{L}\hat{f}_0(k)\exp(ikx + i[\tilde{\omega}_0(\varepsilon k) + \mathcal{O}(\varepsilon^4 k^4)]t/\varepsilon)\,\mathrm{d}k + \mathcal{O}(\varepsilon) \qquad (2.41)$$

$$= \frac{1}{2}\int_{-L}^{L}\hat{f}_0(k)\exp(ikx + i\tilde{\omega}_0(\varepsilon k)t/\varepsilon)\,\mathrm{d}k + \mathcal{O}(\varepsilon^3 t) + \mathcal{O}(\varepsilon) \qquad (2.42)$$

$$=: \tilde{u}_0(x,t) + \mathcal{O}(\varepsilon^3 t) + \mathcal{O}(\varepsilon). \qquad (2.43)$$

Let us now differentiate the leading term $\tilde{u}_0(x,t)$ twice with respect to t,

$$\partial_{tt}\tilde{u}_0(x,t) = \frac{1}{2}\int_{-L}^{L} -\frac{1}{\varepsilon^2}\left(\tilde{\omega}_0(\varepsilon k)\right)^2 \hat{f}_0(k)\exp(ikx + i\tilde{\omega}_0(\varepsilon k)t/\varepsilon)\,\mathrm{d}k \qquad (2.44)$$

and upon expanding the square of $\tilde{\omega}_0$ under the integral we obtain

$$\partial_{tt}\tilde{u}_0(x,t) = -\frac{1}{2}\int_{-L}^{L}\Big[\varepsilon^{-2}\omega_0(0)^2 2\varepsilon^{-1}k\omega_0(0)\omega_0'(0) \qquad (2.45)$$

$$+\frac{1}{2}k^2\left(2\omega_0(0)\omega_0''(0) + 2(\omega_0'(0))^2\right) \qquad (2.46)$$

$$+\frac{1}{6}\varepsilon k^3\left(2\omega_0(0)\omega_0^{(3)}(0) + 6\omega_0'(0)\omega_0''(0)\right) \qquad (2.47)$$

$$+\frac{1}{24}\varepsilon^2 k^4\left(8\omega_0'(0)\omega_0^{(3)}(0) + 6(\omega_0''(0))^2\right) \qquad (2.48)$$

$$+\frac{1}{6}\varepsilon^3 k^5\left(\omega_0''(0)\omega_0^{(3)}(0)\right) + \frac{1}{36}\varepsilon^4 k^6(\omega_0^{(3)}(0))^2\Big]\times \qquad (2.49)$$

$$\hat{f}_0(k)\exp(ikx + i\tilde{\omega}_0(\varepsilon k)t/\varepsilon)\,\mathrm{d}k. \qquad (2.50)$$

We now again use the facts that $\omega_0(0) = 0$ and that by symmetry all odd derivatives of $\omega_0^2(k)$ are zero when evaluated at $k = 0$. Then the expression for $\partial_{tt}\tilde{u}_0$ simplifies to

$$\partial_{tt}\tilde{u}_0(x,t) = -\frac{1}{2!}\int_{-L}^{L}\Big[\frac{1}{2}k^2\left.\frac{\partial^2\omega_0^2(k)}{\partial k^2}\right|_{k=0} + \frac{1}{4!}\varepsilon^2 k^4\left.\frac{\partial^4\omega_0^2(k)}{\partial k^4}\right|_{k=0}$$

$$+\varepsilon^3 k^5 R_1 + \varepsilon^4 k^6 R_2\Big]\hat{f}_0(k)\exp(ikx + i\tilde{\omega}_0(\varepsilon k)t/\varepsilon)\,\mathrm{d}k$$

$$= \frac{1}{2!}\left.\frac{\partial^2\omega_0^2(k)}{\partial k^2}\right|_{k=0}\partial_{xx}\tilde{u}_0(x,t) - \varepsilon^2\frac{1}{4!}\left.\frac{\partial^4\omega_0^2(k)}{\partial k^4}\right|_{k=0}\partial_{xxxx}\tilde{u}_0(x,t)$$

$$- i\varepsilon^3 R_1\partial_{xxxxx}\tilde{u}_0(x,t) - \varepsilon^4 R_2\partial_{xxxxxx}\tilde{u}_0(x,t), \qquad (2.51)$$

where R_1 and R_2 are some real numbers. This is approximated in [49] with the PDE

$$\tilde{u}_{tt} = \bar{A}\tilde{u}_{xx} + \beta\varepsilon^2\tilde{u}_{xxxx}, \qquad (2.52)$$

where

$$\bar{A} = \frac{1}{2!}\left.\frac{\partial^2\omega_0^2}{\partial k^2}\right|_{k=0}, \qquad \beta = -\frac{1}{4!}\left.\frac{\partial^4\omega_0^2}{\partial k^4}\right|_{k=0}. \qquad (2.53)$$

The remaining $m \geq 1$ terms in (2.33) are as we said uniformly bounded by $\mathcal{O}(\varepsilon)$ in L^2-norm, so that we can use $\tilde{u} \approx \tilde{u}_0$ as an $\mathcal{O}(\varepsilon)$ approximation up to the time $t = \mathcal{O}(\varepsilon^{-2})$.

2.6   Geometrical Optics

In this section we will give a brief outline of the theory of classical geometrical optics (GO). GO considers single wave solutions to

$$
\begin{cases}
u_{tt}^{\varepsilon} - \nabla \cdot (a^2 \nabla u^{\varepsilon}) = 0, & \Omega \times [0, T], \\
u^{\varepsilon}(x, 0) = u_0^{\varepsilon}(x), \quad u_t^{\varepsilon}(x, 0) = u_1^{\varepsilon}(x), & \forall x \in \Omega,
\end{cases}
\tag{2.54}
$$

of the form,

$$
u^{\varepsilon}(x, t) = \exp(i\phi(x, t)/\varepsilon) \sum_{k=0}^{\infty} A_k(x, t)(i\varepsilon)^k := \exp(i\phi(x, t)/\varepsilon)\mathcal{A}(x, t).
\tag{2.55}
$$

By inserting (2.55) into (2.54) and collecting terms with equal powers of ε, we obtain equations for the unknowns ϕ and A_k. The equation for the phase ϕ is the so called eikonal equation and the equations for the amplitudes A_k are transport equations. The geometrical optics approximation is common in electromagnetic, elastic and acoustic wave propagation [27].

The (formal) series expansion in (2.55) is called a WKB approximation or the WKB method [36]. It is a general method to find approximations to highly oscillating solutions of (linear) partial differential equations where the coefficients vary in space. The WKB method is named after the three physicists Wentzel, Kramers, and Brillouin, who jointly developed it in 1926. The expansion itself does not in general converge, but can still provide us with insight on how to pick good approximations to the solution u^{ε}.

In the one-dimensional case, we have

$$
\begin{cases}
u_t^{\varepsilon} = \exp(i\phi/\varepsilon)\left[\dfrac{i\phi_t}{\varepsilon}\mathcal{A} + \mathcal{A}_t\right] = \dfrac{i\phi_t}{\varepsilon}u^{\varepsilon} + \exp(i\phi/\varepsilon)\mathcal{A}_t, \\[2mm]
u_x^{\varepsilon} = \exp(i\phi/\varepsilon)\left[\dfrac{i\phi_x}{\varepsilon}\mathcal{A} + \mathcal{A}_x\right] = \dfrac{i\phi_x}{\varepsilon}u^{\varepsilon} + \exp(i\phi/\varepsilon)\mathcal{A}_x,
\end{cases}
\tag{2.56}
$$

and

$$
\begin{cases}
u_{tt}^{\varepsilon} = \exp(i\phi/\varepsilon)\left[\mathcal{A}_{tt} + \dfrac{i\phi_{tt}}{\varepsilon}\mathcal{A} + \dfrac{2i\phi_t}{\varepsilon}\mathcal{A}_t - \dfrac{\phi_t^2}{\varepsilon^2}\mathcal{A}\right], \\[3mm]
u_{xx}^{\varepsilon} = \exp(i\phi/\varepsilon)\left[\mathcal{A}_{xx} + \dfrac{i\phi_{xx}}{\varepsilon}\mathcal{A} + \dfrac{2i\phi_x}{\varepsilon}\mathcal{A}_x - \dfrac{\phi_x^2}{\varepsilon^2}\mathcal{A}\right],
\end{cases}
\tag{2.57}
$$

which gives us that,

$$
\partial_x(a^2 u_x^{\varepsilon}) = 2aa' u_x^{\varepsilon} + a^2 u_{xx}^{\varepsilon} = \exp(i\phi/\varepsilon)
$$
$$
\times \left[\frac{2iaa'\phi_x}{\varepsilon}\mathcal{A} + 2aa'\mathcal{A}_x + a^2\mathcal{A}_{xx} + \frac{ia^2\phi_{xx}}{\varepsilon}\mathcal{A} + \frac{2ia^2\phi_x}{\varepsilon}\mathcal{A}_x - \frac{a^2\phi_x^2}{\varepsilon^2}\mathcal{A}\right].
\tag{2.58}
$$

By plugging in the expansions of u_{tt}^{ε} and $\partial_x(a^2 u_x^{\varepsilon})$ into (2.54) and collecting powers of ε we get a set of equations of the form:

$$\frac{1}{\varepsilon^2} : \quad -\phi_t^2 A_0 + a^2 \phi_x^2 A_0 = 0, \tag{2.59}$$

$$\frac{i}{\varepsilon} : \quad \begin{aligned} \phi_{tt} A_0 + 2\phi_t (A_0)_t - \phi_t^2 A_1 - 2aa'\phi_x A_0 - a^2 \phi_{xx} A_0 \\ -2a^2 \phi_x (A_0)_x + a^2 \phi_x^2 A_1 = 0, \end{aligned} \tag{2.60}$$

$$\varepsilon^k : \quad \begin{aligned} (A_k)_{tt} - (a^2 (A_k)_x)_x + 2\phi_t (A_{k+1})_t - 2a^2 \phi_x (A_{k+1})_x \\ + (\phi_{tt} - (a^2 \phi_x)_x) A_{k+1} + A_{k+2}(-\phi_t^2 + a^2 \phi_x^2) = 0, \end{aligned} \quad k \geq 0. \tag{2.61}$$

The equation for $1/\varepsilon^2$ gives us the eikonal equation

$$\phi_t^2 - a^2 \phi_x^2 = 0 \quad \Leftrightarrow \quad \phi_t = \pm a\phi_x. \tag{2.62}$$

We use the fact that $-\phi_t^2 A_1 + a^2 \phi_x^2 A_1 = 0$, to get the equation corresponding to the i/ε terms,

$$\phi_{tt} A_0 + 2\phi_t (A_0)_t - 2aa'\phi_x A_0 - a^2 \phi_{xx} A_0 - 2a^2 \phi_x (A_0)_x = 0, \tag{2.63}$$

which can be expressed as,

$$\begin{aligned} (A_0)_t &= \frac{-\phi_{tt} + 2aa'\phi_x + a^2 \phi_{xx}}{2\phi_t} A_0 + \frac{a^2 \phi_x}{\phi_t}(A_0)_x \\ &= \frac{(a^2 \phi_x)_x - \phi_{tt}}{2\phi_t} A_0 \pm a(A_0)_x, \\ &= \pm \frac{a'}{2} A_0 \pm a(A_0)_x, \end{aligned} \tag{2.64}$$

where we used the fact that,

$$\begin{aligned} \phi_{tt} = (\pm a\phi_x)_t &= \pm a(\phi_t)_x = \pm a(\pm a\phi_x)_x \\ &= aa'\phi_x + a^2 \phi_{xx} = (a^2 \phi_x)_x - aa'\phi_x = (a^2 \phi_x)_x \mp a'\phi_t. \end{aligned} \tag{2.65}$$

As the final step, to get the equation on conservative form, we multiply both sides with $2A_0$,

$$2A_0 (A_0)_t = \pm a' A_0^2 \pm 2aA_0 (A_0)_x = \pm (a A_0^2)_x. \tag{2.66}$$

The same computations can be made by matching terms for ε^k $(k \geq 0)$,

$$(A_{k+1})_t = \pm \frac{a'}{2} A_{k+1} \pm a(A_{k+1})_x - \frac{(A_k)_{tt} - (a^2 (A_k)_x)_x}{2\phi_t}, \tag{2.67}$$

and by multiplying with $2A_{k+1}$ we get the conservative form,

$$(A_{k+1}^2)_t = \pm (a A_{k+1}^2)_x - \frac{(A_k)_{tt} - (a^2 (A_k)_x)_x}{\phi_t} A_{k+1}. \tag{2.68}$$

In conclusion, we have,

$$
\begin{cases}
\phi_t \pm a\phi_x = 0, \\
(A_0^2)_t \pm (aA_0^2)_x = 0, \\
(A_{k+1}^2)_t \pm (aA_{k+1}^2)_x + \dfrac{(A_k)_{tt} - (a^2(A_k)_x)_x}{\phi_t} A_{k+1} = 0, \quad k \geq 0.
\end{cases}
\tag{2.69}
$$

where the $\pm$ sign should be matched, either we have a plus sign or we have a minus on all equations at the same time. The initial data given by $u_0^\varepsilon(x) = A(x,0)e^{i\phi(x,0)/\varepsilon}$ leads to the initial conditions:

$$
\begin{cases}
\phi(x,0) = \pm\dfrac{\varepsilon}{i}\log\left(\dfrac{u^\varepsilon(x,0)}{|u^\varepsilon(x,0))|}\right), \\
A_0^2(x,0) = |u^\varepsilon(x,0)|^2, \\
A_{k+1}^2(x,0) = 0, \qquad k \geq 0.
\end{cases}
\tag{2.70}
$$

Remark 3. *In the one-dimensional case the fact that the initial data for the phase solves $\phi_x(x,0) = \pm 1/a(x)$ implies that the solution to the eikonal equation (2.62) is very simple, namely $\phi(x,t) = \phi(x,0) \pm t$. The solution will have a plus sign for the right going phase and a minus sign for the left going phase. We call this kind of ϕ a matched phase for $a(x)$.*

2.7 Kernels

In this section we will describe a way to compute averages of oscillatory variables in an efficient way. For the sake of simplifying the notation we will describe the case for one dimensional time and space dependent variables v^ε. All arguments can be extended to any number of dimensions in space.

In the HMM methods we will construct, there is often reason to sample some locally periodic quantity $v^\varepsilon = v(x, x/\varepsilon, t, t/\varepsilon)$, where $v(x, \xi, t, \varphi)$ is periodic in ξ and φ. Assuming the period is one in both ξ and φ, we can obtain the local mean value by $\bar{v}(x,t) = \iint v(x, \xi, t, \varphi)\,d\xi\,d\varphi$ of v^ε, over one period. Note that all integrals are taken over $\mathbb{R}$ if the bounds are not specified.

We will compute $\bar{v}$ using a numerical method. If we know the periodicity of v^ε in both ξ and φ we can compute $\bar{v}$ with spectral accuracy by the trapezoidal rule. The situation becomes harder when we don't know the exact period in one or both oscillatory variables. Suppose we have v^ε over some domain $(x,t) \in [-\eta, \eta] \times [-\tau, \tau]$ where both η and τ are of order ε. We have,

$$
\left| \bar{v} - \frac{1}{4\eta\tau} \int_{-\tau}^{\tau} \int_{-\eta}^{\eta} v^\varepsilon(\xi, s)\,d\xi\,ds \right| \leq C\left(\frac{\varepsilon}{\eta} + \frac{\varepsilon}{\tau}\right).
\tag{2.71}
$$

In general η and τ will be proportional to ε^γ for some real number γ. This mean value computation can be seen as a convolution,

$$\frac{1}{4\eta\tau}\int_{-\tau}^{\tau}\int_{-\eta}^{\eta}v^\varepsilon(\xi,s)\,\mathrm{d}\xi\,\mathrm{d}s = \frac{1}{\eta\tau}\iint \chi_D\left(\frac{\xi}{\eta}\right)\chi_D\left(\frac{\varphi}{\tau}\right)v^\varepsilon(x-\xi,t-\varphi)\,\mathrm{d}\xi\,\mathrm{d}\varphi, \tag{2.72}$$

$$= \iint K_\eta(\xi)K_\tau(\varphi)v^\varepsilon(x-\xi,t-\varphi)\,\mathrm{d}\xi\,\mathrm{d}\varphi \tag{2.73}$$

$$=: (\mathcal{K}v^\varepsilon)(x,t), \tag{2.74}$$

where $D = [-1,1]$, $K_\eta(x) = (1/\eta)K(x/\eta)$, $K_\tau(t) = (1/\tau)K(t/\tau)$, $K = \chi_D$ and χ_D is the scaled characteristic function for the domain D,

$$\chi_D(s) = \begin{cases} \frac{1}{|D|}, & s \in D, \\ 0, & \text{otherwise.} \end{cases} \tag{2.75}$$

We will from here on assume that we use the same kernel K for both time and space variables and that $\eta \sim \tau$ with respect to ε. We will extend the idea of smoothing v^ε with a kernel K to a general class of kernels K:
A kernel $K \in \mathbb{K}^{p,q}$ should satisfy the following conditions:

$$\begin{cases} \displaystyle\int_{\mathbb{R}} K(s)\,\mathrm{d}s = 1, \quad \operatorname{supp} K = [-1,1], \\ \displaystyle\int_{\mathbb{R}} s^i K(s)\,\mathrm{d}s = 0, \quad 1 \le i \le p, \\ \displaystyle\frac{\mathrm{d}^i K(s)}{\mathrm{d}s^i} = 0, \quad 0 \le i \le q, \quad \text{for both } s = -1 \text{ and } s = 1. \end{cases} \tag{2.76}$$

From [31] we have the following result:

Theorem 4. *Let $X^\varepsilon(t) = X(t,\frac{t}{\varepsilon})$, where X is 1-periodic in the second variable and $\frac{\partial^r X(t,s)}{\partial t^r}$ is continuous for $r = 0,1,\ldots,p-1$. For any $K \in \mathbb{K}^{p,q}$ there exists constants C_1 and C_2, independent of ε and η such that,*

$$|(K_\eta * X^\varepsilon)(t) - Y(t)| \le C_1\left(\frac{\varepsilon}{\eta}\right)^q + C_2\eta^p, \tag{2.77}$$

where $K_\tau(x) = (1/\tau)K(\frac{t}{\tau})$ and $Y(t) = \int_0^1 X(t,s)\,\mathrm{d}s$.

The convergence rate in (2.71) with respect to η and τ improves if we use a kernel $K \in \mathbb{K}^{p,q}$ with compact support and that is q times continuously differentiable. Define the scaling $K_\Omega(x) := \frac{1}{\Omega}K(\frac{x}{\Omega})$. We have,

$$\left|\bar{v}(x,t) - \iint K_\eta(\xi)K_\tau(\varphi)v^\varepsilon(x-\xi,t-\varphi)\,\mathrm{d}\xi\,\mathrm{d}\varphi\right|$$

$$= |\bar{v}(x,t) - (\mathcal{K}v^\varepsilon)(x,t)| \le C\left(\left(\frac{\varepsilon}{\eta}\right)^q + \left(\frac{\varepsilon}{\tau}\right)^q + \eta^p + \tau^p\right). \tag{2.78}$$

We have chosen to work with the kernel space $\mathbb{K}^{p,q}$ which contains functions that are polynomials on $[-1, 1]$ and zero outside $[-1, 1]$. We also demand that the kernel functions are q times continuously differentiable and zero on the boundary and with p zero moments, i.e., $\int K(x)x^i \, \mathrm{d}x = 0$, $1 \leq 1 \leq p$, and with integral $\int K(x) \, \mathrm{d}x = 1$. One can show that all kernels K in $\mathbb{K}^{p,q}$ are of the form

$$K(x) = (1 - x^2)^{q+1} P(x), \tag{2.79}$$

where $P(x)$ is a degree p polynomial. We have supplied a code in [34] which computes the coefficients of P in $K(x) = (1 - x^2)^{q+1} P(x)$ for any $K \in \mathbb{K}^{p,q}$. An example why it is important for the numerical accuracy to factorize the polynomial on the form $K(x) = (1 - x^2)^{q+1} P(x)$ is shown in Tab. 2.1.

Remark 5. *We will often make use of the fact that the operator $\mathcal{K}$ commutes with ∂_t and ∂_x. We observe that,*

$$\partial_t \mathcal{K} v^\varepsilon = \iint K_\eta(\xi) K_\tau(\varphi) \partial_t v^\varepsilon(x - \xi, t - \varphi) \, \mathrm{d}\xi \, \mathrm{d}\varphi = \mathcal{K} v_t^\varepsilon, \tag{2.80}$$

and similarly for ∂_x.

N \ $K(x)$	14 terms $7475.95 \cdots x^{28} + \cdots$	$(1 - x^2)^{q+1} P(x)$
10	6.0572e-04	6.0572e-04
20	1.5465e-07	1.5467e-07
40	2.2333e-10	2.6219e-10
80	3.6733e-11	8.3822e-14
160	4.8612e-11	1.1102e-16

Table 2.1: A table of the quadrature error $|1 - \Delta x \sum_{i=0}^{N} K(x_i)|$ as a function of the grid size N for two ways of evaluating the integral of the same polynomial $K \in \mathbb{K}^{9,9}$. The polynomial evaluations are done with Horner's method with the Matlab built-in function `polyval`. We clearly see that there is a great benefit in using the factorized K from a numerical perspective. The 28 degree polynomial K has only even powers of x^i, but has very large coefficients. The large coefficients and the number of terms makes it difficult to evaluate K accurately. The expected convergence rate is spectral.

Remark 6. *It is possible to find functions with infinite q. In [31] a kernel $K_{\exp}$ is given, where $p = 1$ and q is infinite:*

$$K_{\exp}(x) = \begin{cases} C_0 \exp\left(\frac{5}{x^2-1}\right), & |x| < 1, \\ 0, & |x| \geq 1, \end{cases} \tag{2.81}$$

where C_0 is chosen such that $\int K_{exp}(x)\,\mathrm{d}x = 1$. This kernel is suitable for problems where A^ε is of the form $A^\varepsilon(x) = A(x/\varepsilon)$.

Chapter 3

Summary of Paper I and II: HMM for Finite Time Wave Propagation Problems

In Paper I and II we consider the following multiscale wave propagation problem:

$$\begin{cases} u_{tt}^\varepsilon - \nabla \cdot (A^\varepsilon \nabla u^\varepsilon) = 0, & \Omega \times [0, T], \\ u^\varepsilon(x, 0) = u_0(x), \quad u_t^\varepsilon(x, 0) = u_1(x), & \forall x \in \Omega, \end{cases} \tag{3.1}$$

where u^ε is Ω-periodic; the initial data and time T is independent of ε; and A^ε is uniformly positive and symmetric.

When A^ε is of the form $A^\varepsilon(x) = A(x, x/\varepsilon)$ and $A(x, y)$ is 1-periodic in y, we observe that the solution u^ε appears to converge to some solution $\bar{u}$. It is also a well known fact that, in the limit, $\varepsilon \to 0$, the solution to (3.1) will approach the solution to another PDE, a *homogenized* PDE (cf. Section 2.4). This fact is illustrated in Figure 3.1. In [21, 24], which we will summarize in this chapter, we developed a multiscale method for the wave equation (3.1) in one, two and three dimensions. The method can easily be extended to higher dimensions as well. We prove that our method converges to the homogenized solution in a setting where homogenization is applicable. We demonstrate that our HMM method give the correct results in cases where the homogenized PDE is unknown. It should be noted that even though our numerical methods use ideas from homogenization theory they do not solve the homogenized equations directly. The goal is to develop computational techniques that can be used when there is no known homogenized equation available. The closed form of the homogenized equation may not be available, for example due to non-periodic coefficients. In the research presented here the homogenized equations are actually available and could in practice self be numerically approximated. We have chosen this case in order to be able to develop a rigorous convergence analysis and to have a well-understood environment for numerical tests.
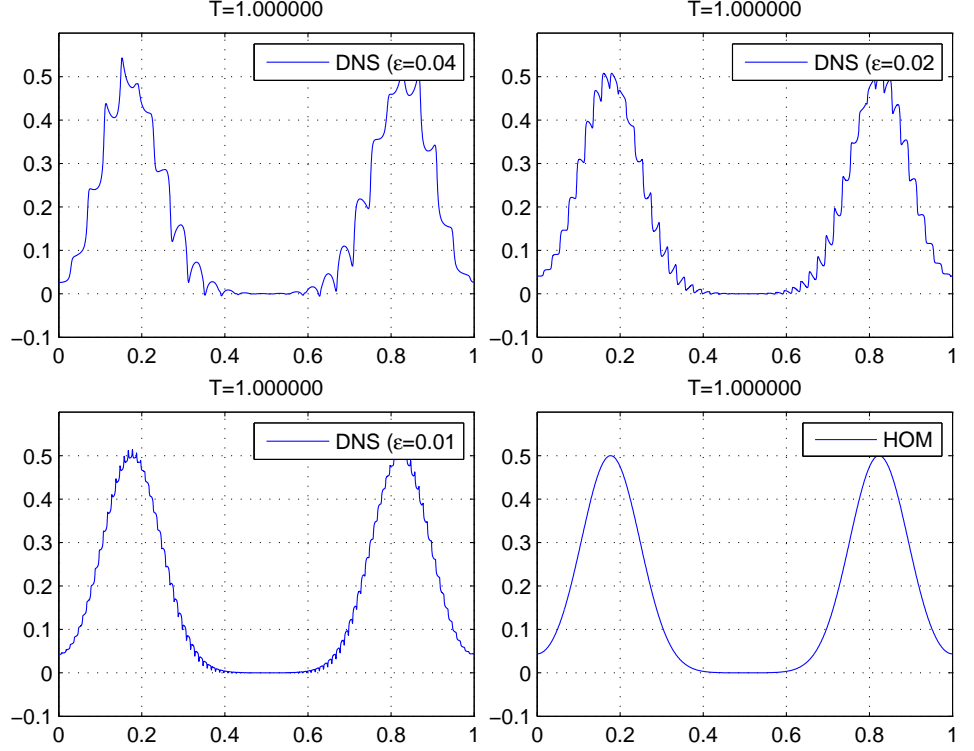
Figure 3.1: A series of solutions for different ε at $T = 1$ for the wave equation with $A^\varepsilon(x) = 1.1 + \sin \frac{2\pi x}{\varepsilon}$ over the domain $\Omega = [0, 1]$; initial data $u_0(x) = \exp(-100(x - 0.5)^2)$, $u_1(x) = 0$; and periodic boundary conditions.

3.1 HMM for the Wave Equation

We will formulate a general HMM framework for the wave equation, (3.1). We follow the same strategy as in [1] for parabolic equations and in [48] for the one-dimensional advection equation. We assume there exists a macroscale PDE of the form

$$\begin{cases} u_{tt} - \nabla \cdot F(x, \nabla u) = 0, & \Omega \times [0, T], \\ u(x, 0) = u_0(x), \quad u_t(x, 0) = u_1(x), & \forall x \in \Omega, \end{cases} \tag{3.2}$$

where u is Ω-periodic. The assumption on (3.2) is that $u \approx u^\varepsilon$ when ε is small. In the pure homogenization case we would have $F = \bar{A}\nabla u$, but we will not assume knowledge of a homogenized equation. Instead we will solve the PDE (3.1), only in a small time and space box, with initial data depending on x and ∇u, and from that solution extract a value for F. The form of the initial data for this micro problem will be determined from the local behavior of u.

In the next chapter we will give an condensed description of the HMM algorithm, found in Algorithm 4.2.

Macro Model Discretization

We discretize (3.2) using central differences with time step K and spatial grid size H in all directions,

$$
\begin{cases}
U_m^{n+1} = 2U_m^n - U_m^{n-1} + \dfrac{K^2}{H} \sum_{k=1}^d \left(e_k^T F_{m+\frac{1}{2}e_k}^n - e_k^T F_{m-\frac{1}{2}e_k}^n \right), \\
F_{m-\frac{1}{2}e_k}^n = F(x_{m-\frac{1}{2}e_k}, P_{m-\frac{1}{2}e_k}^n), \qquad 1 \le k \le d,
\end{cases}
\tag{3.3}
$$

where $F_{m\pm\frac{1}{2}e_k}^n$ is the vector F evaluated at point $x_{m\pm\frac{1}{2}e_k}$. The quantity $P_{m\pm\frac{1}{2}e_k}^n$ approximates $\nabla u(t_n, x_{m\pm\frac{1}{2}e_k})$. In Figure 3.2 we show an example of the numerical scheme for P in two dimensions. The macro discretization H and K is supposed to be fine enough to capture all information on the macroscopic scale. We refer to [24, 34] for further details about the numerics and implementation.

Micro Problem and Reconstruction Operator

The evaluation of $F_{m-\frac{1}{2}e_k}^n$ in each grid point is done by solving a micro problem to fill in the missing data in the macro model. Given the parameters $x_{m-\frac{1}{2}e_k}$ and $P_{m-\frac{1}{2}e_k}^n$, we solve a corresponding micro problem over a small micro box Y^ε, centered around $x_{m-\frac{1}{2}e_k}$. In order to simplify the notation, we make a change of variables $x - x_{m-\frac{1}{2}e_k} \mapsto x$ and $t - t_n \mapsto t$. This implies that $A^\varepsilon(x) \mapsto A^\varepsilon(x + x_{m-\frac{1}{2}e_k})$. The micro problem has the form,

$$
\begin{cases}
v_{tt}^\varepsilon - \nabla \cdot (A^\varepsilon \nabla v^\varepsilon) = 0, & Y^\varepsilon \times [-\tau, \tau], \\
v^\varepsilon(x, 0) = (P_{m-\frac{1}{2}e_k}^n) \cdot x, \quad v_t^\varepsilon(x, 0) = 0, & \forall x \in Y^\varepsilon.
\end{cases}
\tag{3.4}
$$

The micro box size should be of order ε, i.e., both τ and $\operatorname{diam} Y^\varepsilon$ are $\mathcal{O}(\varepsilon)$ since the computational cost of solving (3.4) should be small compared to solving the entire wave equation (3.1), as noted in [18],

$$
\frac{\text{cost of multiscale method}}{\text{cost of microscale solver on entire domain}} \ll 1.
\tag{3.5}
$$

We note that the solution v^ε is an even function with respect to t, i.e., $v^\varepsilon(x, -t) = v^\varepsilon(x, t)$, due to the initial condition $v_t^\varepsilon(x, 0) = 0$. Thus, it is only needed to solve (3.4) for positive t.

Compression Operator

After we have solved for v^ε for all $Y^\varepsilon \times [-\tau, \tau]$ we approximate

$$
F_{m-\frac{1}{2}e_k}^n \approx \tilde{F}(x_{m-\frac{1}{2}e_k}, P_{m-\frac{1}{2}e_k}^n),
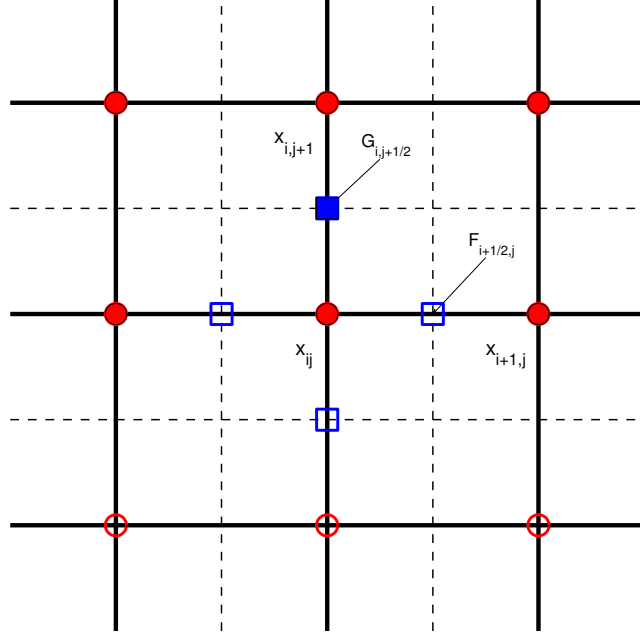\tag{3.6}
$$

Figure 3.2: The numerical scheme (3.3) for P in two dimensions. The two components of F in two different positions are given by $F_{i+1/2,j}$ and $G_{i,j+1/2}$. The U points involved in computing $F^n_{m+\frac{1}{2}e_2} = G_{i,j+1/2}$ and $\nabla u \approx P^n_{m+\frac{1}{2}e_2}$ are indicated by filled circles. Note that the squares are where either $(A^\varepsilon_{11}\partial_x + A^\varepsilon_{12}\partial_y)u^\varepsilon$ or $(A^\varepsilon_{21}\partial_x + A^\varepsilon_{22}\partial_y)u^\varepsilon$ are computed, and not the full gradient $A^\varepsilon\nabla u^\varepsilon$.

where function $\tilde{F}$ is the mean value of $f^\varepsilon = A^\varepsilon\nabla v^\varepsilon$ over $[-\eta,\eta]^d \times [-\tau,\tau]$ and $[-\eta,\eta]^d \subset Y^\varepsilon$. The approximation can be improved with respect to the size of ε/τ and ε/η, by computing a weighted average of f^ε. We consider kernels $K \in \mathbb{K}^{p,q}$ described in Section 2.7. We use kernels of this sort to improve the approximation quality for the mean value computation,

$$\tilde{F}(x_{m-\frac{1}{2}e_k}, P^n_{m-\frac{1}{2}e_k}) = \iint K_\tau(t)K_\eta(x)f^\varepsilon_k \, \mathrm{d}x \, \mathrm{d}t, \qquad (3.7)$$

where

$$f^\varepsilon_k(x,t) = A^\varepsilon(x + x_{m-\frac{1}{2}e_k})\nabla v^\varepsilon(x,t) \qquad (3.8)$$

and the multi-variable kernel $K_\eta(x)$ is defined as,

$$K_\eta(x) = K_\eta(x_1)K_\eta(x_2)\cdots K_\eta(x_d), \qquad (3.9)$$

using the single valued kernel K_η, still denoted by K_η. The domain Y^ε is chosen such that $[-\eta,\eta]^d \subset Y^\varepsilon$ and sufficiently large for information not to propagate into

the region $[-\eta, \eta]^d$. Typically we use

$$Y = [-y_{\max}, y_{\max}]^d, \qquad y_{\max} = \eta + \tau \sqrt{\sup \|A^\varepsilon\|_2}, \qquad (3.10)$$

cf. discussion about micro solver boundary conditions in [48]. In this way we do not need to worry about the effects of boundary conditions. Note therefore that other types of boundary conditions could also be used in (3.4).

Remark 7. *The weighted integrals in Section 3.1 are computed numerically with the trapezoidal rule in time and the midpoint rule in space.*

Remark 8. *In our implementation, the micro problem (3.4) is solved with the same numerical scheme as the macro problem (3.3) with a discrete approximation of $f^\varepsilon = A^\varepsilon \nabla v^\varepsilon$ [24].*

3.2 Elements of the Method

In the following two sections we will consider the computational complexity of the method we just described as well as convergence. This is done in a restricted setting where we can compare with a known macroscopic equation from homogenization.

Computational Cost

We will now discuss an alternative to computing (3.7) on-the-fly in the macro solver. In some cases, when the dimension and the number of parameters in the problem are few, a sequential coupling can prove to be more efficient. We stress that the algorithm suggested here does not *require* precomputing and all analysis are made for on-the-fly computations.

Let us assume that the time step is proportional to ε in all direct solvers. Using a direct solver for (3.1) on the full domain implies a cost of order $\varepsilon^{-(d+1)}$. The total cost for on-the-fly HMM is of the form (cost of micro problem) $\times M_d$ where

$$M_d \sim \frac{1}{K} \cdot \frac{1}{H^d} \qquad (3.11)$$

is the number of micro problems needed to be solved. The cost of a single micro problem is of the form $(\tau/\varepsilon) \times (\eta/\varepsilon)^d$. We assume kernels with $\tau, \eta \sim \varepsilon$ and that M_d does not depend on ε. With these assumption our HMM method has a computational cost independent of ε. The constant can, however, still be large as it is proportional to M_d which depends inversely on K and H^d. Fortunately the computational cost of the HMM process can be reduced significantly. We observe that the function $\tilde{F}(x, p)$ in (3.7) is linear in p. It is in fact composed of three linear operations:

1. Compute initial data $v(x, 0) = p \cdot x$ and $v_t(x, 0) = 0$.

2. Solve $v_{tt}^\varepsilon - \nabla \cdot (A^\varepsilon \nabla v^\varepsilon) = 0$ for $-\tau \leq t \leq \tau$.

3. Compute average $\tilde{F} = \iint K_\tau K_\eta f^\varepsilon \, \mathrm{d}x \, \mathrm{d}t$ where $f^\varepsilon = A^\varepsilon \nabla v^\varepsilon$.

The first operation is clearly a linear operation. In step two we compute a solution to a linear PDE, therefore this step is linear as well. Computing the integral average in step three is also a linear operation.

As a corollary we can apply the HMM process to a smaller number of micro problems and form linear combinations of those for any given $\tilde{F}$ computation. More precisely, after precomputing $\tilde{F}(x, e_i)$, $i = 1, 2, \ldots, d$ we can compute $\tilde{F}$ for fixed $x \in \Omega$ and any $p \in \mathbb{R}^d$,

$$\tilde{F}(x, p) = \sum_{i=1}^{d} p_i \tilde{F}(x, e_i), \tag{3.12}$$

where p_i is the ith coefficient in p in the basis $e_1, e_2, \ldots, e_d$. In conclusion, by precomputing the micro problems $\tilde{F}(x_m, e_i)$ in (3.12) we only need to solve d micro problems in each macro grid point x_m. There is no need to solve any micro problems again in the next macro time step. The complexity is as before $\mathcal{O}(1)$ in ε, but now $M_d \sim d/H^d$ which means a smaller constant not depending on the number of time steps. Note that this works if A^ε does not depend on t. If A^ε depends on t or is nonlinear in u it would in general not be as cost effective to precompute $\tilde{F}$.

Remark 9. *In fact, if A^ε is ε-periodic and the macro grid is such that $x_m = r$ (mod ε), where r is constant and independent of m, we only need to solve d micro problems in total, i.e., $M_d = d$. In this case, the total cost is independent of both ε and the macro grid sizes H, K.*

Remark 10. *The flux computations in the macro scheme suggested here is embarrassingly parallel in space. This fact has been exploited by the authors in a Message Passing Interface (MPI) code. We think that it would be possible to implement the same algorithm in a general purpose GPU environment and see a good utilization of the hardware.*

Convergence Theory

In this section we apply the HMM process to the problem (3.1) with $A^\varepsilon(x) = A(x/\varepsilon)$ where A is a Y-periodic symmetric positive matrix and show that it generates results close to a direct discretization of the homogenized equation (2.12). We will show a convergence result for smooth (i.e., C^∞) solutions and data. In particular we show that

$$\tilde{F}(x, p) = F(x, p) + \mathcal{O}\left(\left(\frac{\varepsilon}{\eta} \right)^q \right). \tag{3.13}$$

The functions $\tilde{F}$ and F are defined in (3.7) and (3.2) respectively and we note that in this case $F(x, p) = \bar{A}p$. The integer q depends on the smoothness of the kernel used to compute the weighted average of f^ε in (3.7).

We will formulate the problem in the setting of elliptic operators. For the analysis we solve the micro problem (3.4) over all of $\mathbb{R}^d$

$$
\begin{cases}
v_{tt}^\varepsilon - \nabla \cdot (A^\varepsilon \nabla v^\varepsilon) = 0, & \mathbb{R}^d \times [-\tau, \tau], \\
v^\varepsilon(x,0) = p \cdot x, \quad v_t^\varepsilon(x,0) = 0, & \forall x \in \mathbb{R}^d.
\end{cases}
\tag{3.14}
$$

Note that this gives the same $\tilde{F}$ as in (3.7) if we choose a sufficiently large box Y^ε.

Theorem 11. *Let $\tilde{F}(x_0, p)$ be defined by (3.7) where v^ε solves the micro problem (3.14) exactly, $A^\varepsilon(x) = A(x/\varepsilon)$ and A is Y-periodic and C^∞. Moreover suppose $K \in \mathbb{K}^{p',q}$, u_0 and u_1 are C^∞ and $\tau = \eta$. Then for $p \neq 0$,*

$$
\frac{1}{p} \left| \tilde{F}(x_0, p) - F(x_0, p) \right| \leq C \left(\frac{\varepsilon}{\eta} \right)^q,
\tag{3.15}
$$

where C is independent of ε, η, p and q. Furthermore, for the numerical approximation given in (3.3) in one dimension, with $H = n\varepsilon$ for some integer n and smooth initial data, we have the error estimate

$$
|U_m^n - \bar{u}(x_m, t_n)| \leq C(T) \left(H^2 + (\varepsilon/\eta)^q \right), \qquad 0 \leq t_n \leq T,
\tag{3.16}
$$

where $\bar{u}$ is the homogenized solution to the corresponding homogenized equation.

The proof can be found in [24].

Convergence Study with Respect to Choice of Kernel

We investigate the effect of the choice of kernel on the solution of the wave equation on a micro box of order ε. We use $A^\varepsilon(x) = A_1(x/\varepsilon)$ and $A^\varepsilon(x) = A_2(x, x/\varepsilon)$ where $A_1(y) = 1.1 + \sin(2\pi y)$ and $A_2(x, y) = 1.1 + \frac{1}{2}(\sin 2\pi x + \sin 2\pi y)$. We compare our numerical results to the theoretical bounds in Theorem 11. On problems with both fast and slow scales, which is not directly covered by Theorem 11, we see a (slow) growth of the error as $\tau, \eta \to \infty$ consistent with the general approximation result in Theorem 4. In Figure 3.3 and 3.4 we present convergence results for the approximate flux $\tilde{F}$ in terms of $\eta/\varepsilon = \tau/\varepsilon$. We have plotted $(\varepsilon/\eta)^q$ and η^p with dashed lines.

3.3 Numerical Results

We will present a numerical computation for a 2d problem of the form

$$
\begin{cases}
u_{tt}^\varepsilon - \nabla \cdot (A^\varepsilon \nabla u^\varepsilon) = 0, & \Omega \times [0, T], \\
u^\varepsilon(x,0) = e^{-10(x_1-0.5)^2} + e^{-10(x_2-0.5)^2}, & u_t^\varepsilon(x,0) = 0, \quad \forall x \in \Omega,
\end{cases}
\tag{3.17}
$$

and Ω-periodic boundary conditions; $\varepsilon = 0.1$; $\Delta x = 0.02$; $\Delta t = 0.005$ for the macro solver (HMM) and the direct solver for the homogenized equation (denoted HOM).
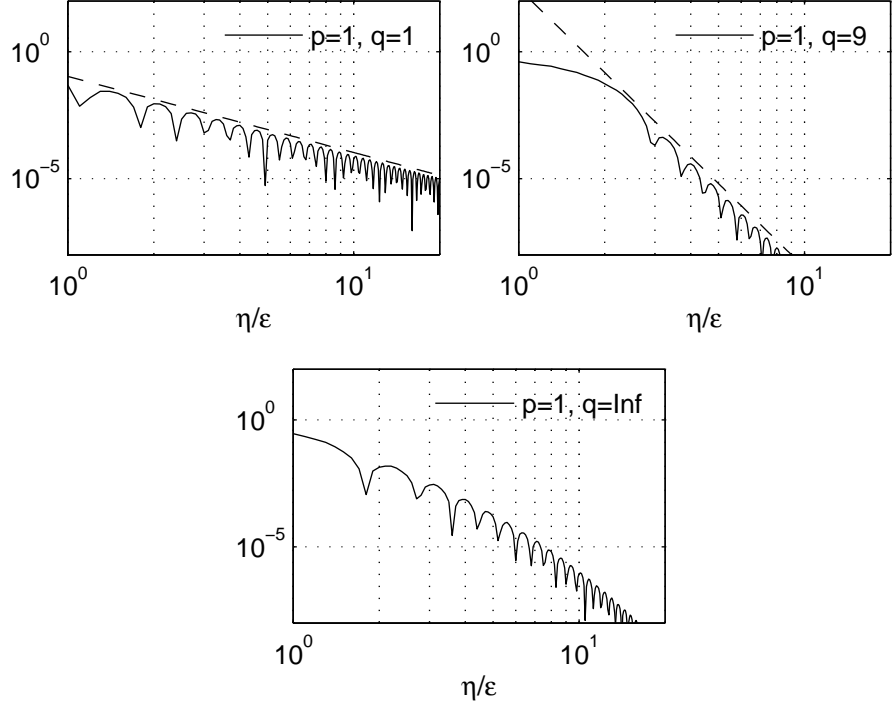
Figure 3.3: Convergence results, error $|\tilde{F} - \bar{F}|$ plotted against η/ε ($\tau = \eta$) for fixed $\varepsilon = 0.01$ and where $A^\varepsilon = A_1$ with only fast scales. The dashed line corresponds to the $(\varepsilon/\eta)^q$ term in Theorem 11. The bottom figure shows results for the exponential kernel (see Remark 6) and indicates super algebraic convergence rate.

For the micro solver and exact (DNS) solver we use; 64 points per wavelength for Δx; $\Delta t = 0.25\Delta x$; and a kernel $K \in \mathbb{K}^{9,9}$. We use the material $A^\varepsilon(x) = A(x, x/\varepsilon)$,

$$A(x,y) = \begin{bmatrix} a(y_1) & 0 \\ 0 & a(y_1) \end{bmatrix}, \quad a(\xi) = 1.1 + \sin 2\pi\xi, \tag{3.18}$$

where the corresponding homogenized $\bar{A}$ will be constant and of the form,

$$\bar{A} = \begin{bmatrix} \sqrt{0.21} & 0 \\ 0 & 1.1 \end{bmatrix}. \tag{3.19}$$

We present a snapshot from $T = 0.5$ in Figs. 3.5, 3.6 and 3.7 for DNS, HOM and HMM computation.
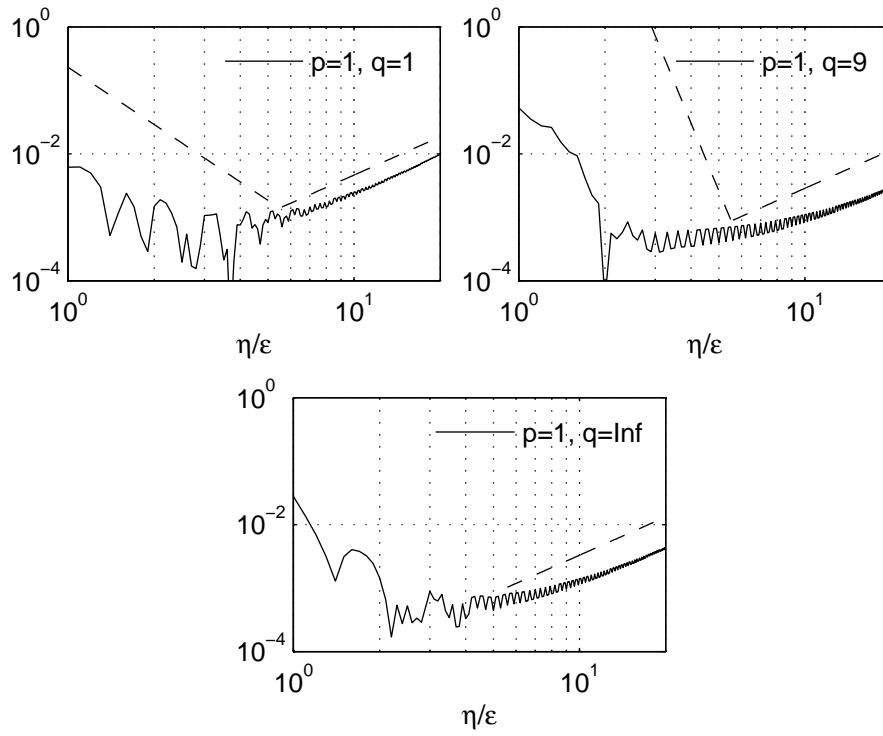
Figure 3.4: Convergence results, error $|\tilde{F} - \bar{F}|$ plotted against η/ε ($\tau = \eta$) for fixed $\varepsilon = 0.01$ and where $A^\varepsilon = A_2$ with both fast and slow scales. The dashed line with negative slope corresponds to the theoretical bound from the first term in Lemma 1 and the dashed line with positive slope corresponds to the η^p term.

Figure 3.5: DNS solution of the 2d problem Section 3.3.

Figure 3.6: HOM solution of the 2d problem Section 3.3.

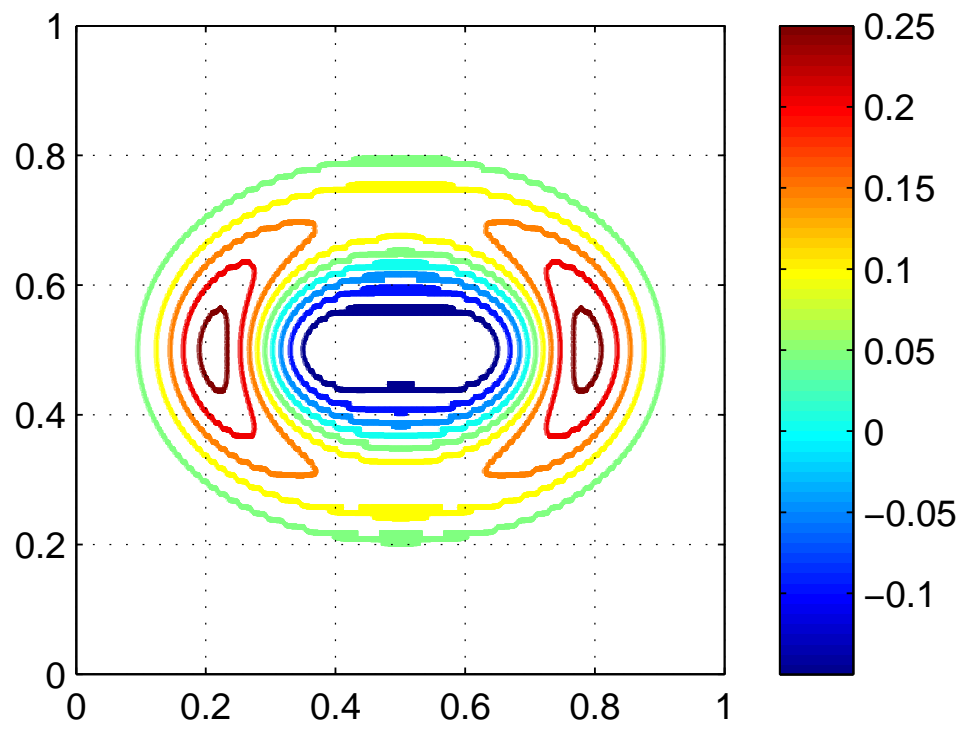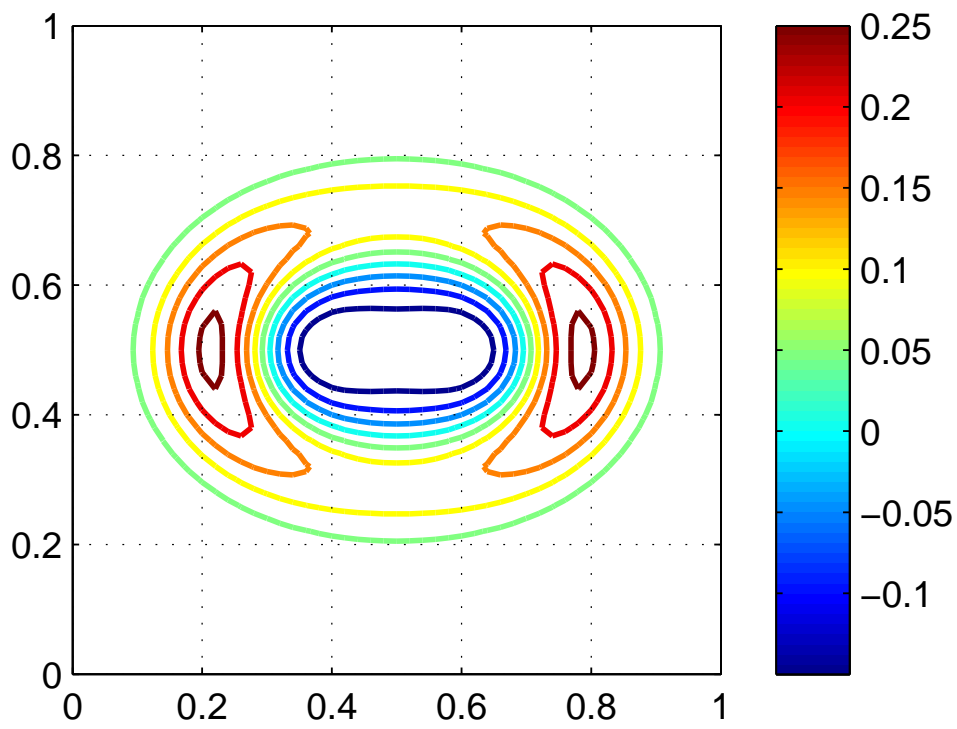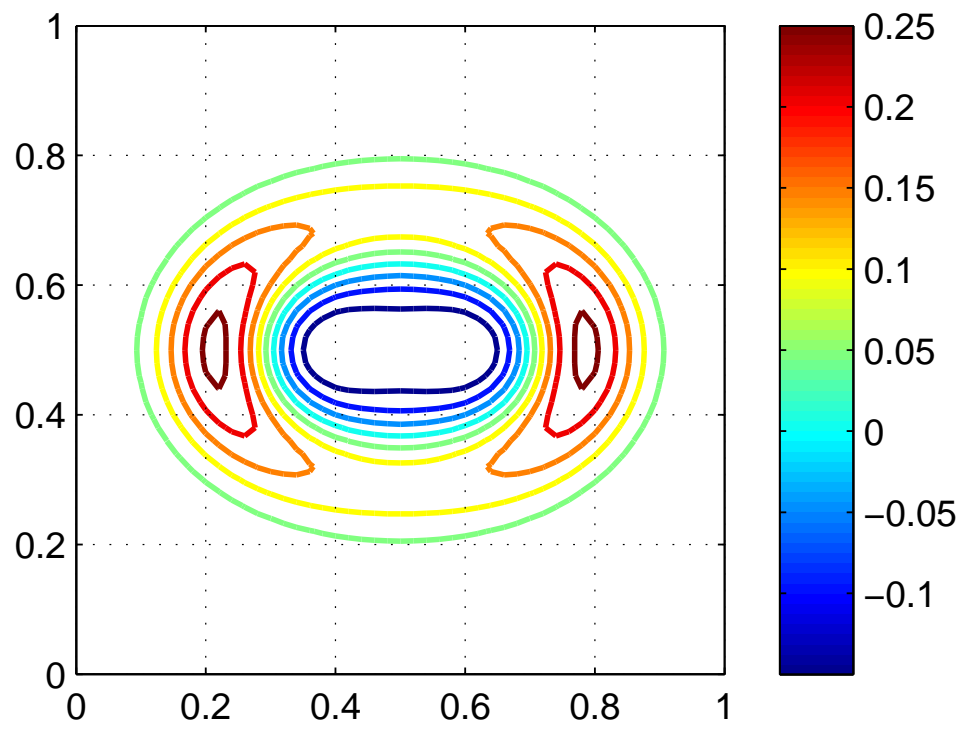Figure 3.7: HMM solution of the 2d problem Section 3.3.

Chapter 4

Summary of Paper III and IV: HMM for Long Time Wave Propagation Problems

In paper III and IV we developed a HMM method for the wave equation for long time,

$$\begin{cases} u_{tt}^{\varepsilon} - \nabla \cdot (A^{\varepsilon} \nabla u^{\varepsilon}) = 0, & \Omega \times [0, T^{\varepsilon}], \\ u^{\varepsilon}(x, 0) = u_0(x), & u_t^{\varepsilon}(x, 0) = u_1(x), \quad \forall x \in \Omega, \end{cases} \tag{4.1}$$

where $T = \mathcal{O}(\varepsilon^{-2})$ and Ω-periodic boundary conditions. The solution of the homogenized problem (2.12) can be used as an approximation to (4.1) when ε is small and for finite time $T^{\varepsilon} = \mathcal{O}(1)$. However, here we assume that $T^{\varepsilon} = \mathcal{O}(\varepsilon^{-2})$, what we will call *long time*. As we saw in Section 2.5 another effective equation is required to capture the dispersive effects that generally is seen in the solution after long time. The dispersive effects are not captured by the standard homogenized wave equation. We described in Section 2.5 an equation by Santosa and Symes [49] which models the dispersive effects that occur after long time. Their effective equation in one-dimension and long time is of the form,

$$\begin{cases} u_{tt} - \bar{A} u_{xx} - \beta \varepsilon^2 u_{xxxx} = 0, & \Omega \times [0, T^{\varepsilon}], \\ u(x, 0) = u_0(x), & u_t(x, 0) = u_1(x), \quad \forall x \in \Omega, \end{cases} \tag{4.2}$$

where $\bar{A}$ is the same as as before and given by classical homogenization theory. The new coefficient, β, is a functional of A and models the dispersion effects generated by the microscale in A^{ε} but its effect is only seen after long time. It should be noted that (4.2) is not well-posed since $\beta > 0$. However, one can solve a regularized equation as we discussed in Section 2.5.

4.1   HMM for the Wave Equation

We will now describe a HMM method for the wave equation (4.1) which will give useful solutions in two regimes. The first regime is when T is fixed and independent of ε. The other regime is when $T^\varepsilon = \mathcal{O}(\varepsilon^{-2})$ and $T^\varepsilon \to \infty$ as $\varepsilon \to 0$. We will call this the *long time* regime and the problem itself a long time wave propagation problem. Here we will consider the one dimensional wave propagation problem. Many of the results can be shown to hold in a d-dimensional setting. We have in previous work shown higher dimensional results, both theoretical and numerical. We demonstrated in [24, 25], summarized in Chapter 3, that our HMM captures the same solution as homogenization (when applicable). In this paper we will primarily investigate how our HMM method handles the long time problem. The microscopic variations in the medium introduces dispersive effects in the macroscopic behavior of the solution which becomes notable after long time. Our goal is to show that our HMM method can capture the dispersion with less computational cost than just resolving the full equation.

The HMM method we suggest here is described in three separate steps. We follow the same strategy as in [1] for parabolic equations and in [48] for the one-dimensional advection equation. See [21], [24] and [2] for additional details and proofs. In step one we give the macroscopic PDE (i.e., $F(U, D) = 0$ in the HMM framework) and a corresponding numerical discretization. In step two we describe the microproblem. The initial data for the microproblem is based on local macroscopic data. Finally, in step three we describe how we approximate F from the computed microproblem by taking a weighted average of its solution.

We consider (4.1) in a one dimensional setting,

$$\begin{cases} u_{tt}^\varepsilon - \partial_x(A^\varepsilon u_x^\varepsilon) = 0, & \Omega \times [0, T^\varepsilon], \\ u^\varepsilon(x,0) = u_0(x), & u_t^\varepsilon(x,0) = u_1(x), \qquad \forall x \in \Omega. \end{cases} \tag{4.3}$$

where $\Omega \subset \mathbb{R}$ is an interval of the form $[a, b]$ and $u^\varepsilon(x, t)$ is Ω-periodic in x. Motivated by the theory in 2.5 we suppose there exists a corresponding macroscale PDE of the form,

$$\begin{cases} u_{tt} - \partial_x F = 0, & \Omega \times [0, T^\varepsilon], \\ u(x,0) = u_0(x), & u_t(x,0) = u_1(x), \qquad \forall x \in \Omega, \end{cases} \tag{4.4}$$

where u is Ω-periodic and $F = F(x, u, u_x, u_{xx}, u_{xxx})$. The assumption on (4.4) is that $u \approx u^\varepsilon$ when ε is small. In the pure homogenization case we would have $F = \bar{A}u_x$, and for the effective equation (2.26) we would have $F = \bar{A}u_x + \beta\varepsilon^2 u_{xxx}$, but we will not assume knowledge of the exact form of a homogenized equation or any other effective equation.

Macro Model Discretization

We discretize (4.4) using central differences with time step K and spatial grid size H in all directions,

$$U_m^{n+1} = 2U_m^n - U_m^{n-1} + \frac{K^2}{24H}\left(-F_{m+3/2}^n + 27F_{m+1/2}^n - 27F_{m-1/2}^n + F_{m-3/2}^n\right). \quad (4.5)$$

where $F_{m-\frac{1}{2}}^n$ is F evaluated at $x_{m-\frac{1}{2}}$. The scheme is second order in K and fourth order in H. We choose to use a fourth order scheme in space because it has better dispersive properties. This allow us to avoid some of the numerical dispersion that pollutes the numerical solution. We will cover how F is computed in the description of the micro problem and refer to [34] for implementation details about the macro model discretization and a dispersion analysis.

Micro Problem and Reconstruction Operator

The evaluation of F in each grid point is done by solving a micro problem to fill in the missing data in the macro model. Given the parameters x' and an initial data $Q(x)$, we solve

$$\begin{cases} v_{tt}^\varepsilon - \partial_x(A^\varepsilon(x + x')v_x^\varepsilon) = 0, & Y^\varepsilon \times [-\tau, \tau], \\ v^\varepsilon(x, 0) = Q(x + x'), \quad v_t^\varepsilon(x, 0) = 0, & \forall x \in Y^\varepsilon, \end{cases} \quad (4.6)$$

where v^ε is Y^ε-periodic and Q depends on the macroscopic state $\{u_m^n\}$, assuming $x' = x_{m-1/2}$, it is typically a piecewise third order polynomial interpolating $u_{m-2}^n, \ldots, u_{m+1}^n$ in $x_{m-2}, \ldots, x_{m+1}$. Note that we have made a change of variables to center Y^ε around x' via $x - x' \mapsto x$ and $t - t' \mapsto t$. We keep the sides of the micro box Y^ε of order ε. We will discuss the choice of Y^ε and Q below.

Compression Operator

After we have solved for v^ε for all $Y^\varepsilon \times [-\tau, \tau]$ we approximate F by a weighted average of the microscopic flux $f^\varepsilon = A^\varepsilon(x + x')v_x^\varepsilon$ over $[-\eta, \eta] \times [-\tau, \tau]$ where $[-\eta, \eta] \subset Y^\varepsilon$. We choose η sufficiently small for information not to have propagated into the region $[-\eta, \eta]$ from the boundary of the micro box Y^ε. More precisely, we consider averaging kernels K described in 2.7. We then approximate

$$F \approx \tilde{F}(x', Q) = \mathcal{K}(f^\varepsilon)(0, 0) = \iint K_\tau(t)K_\eta(x)f^\varepsilon(x, t)\,\mathrm{d}x\,\mathrm{d}t, \quad (4.7)$$

where $f^\varepsilon(x, t) = A^\varepsilon(x + x')v_x^\varepsilon(x, t)$ and v^ε solves (4.6). The choice of kernel has been discussed in Section 2.7. Finally, we give a brief summary of the algorithm in Algorithm 4.2.

Motivation of the Method

Let us define $u(x,t) = (\mathcal{K}u^\varepsilon)(x,t)$ as the course scale variation of u^ε. We will show that u satisfy a PDE of the form $u_{tt} - \partial_x F = 0$. We consider the wave equation (4.3). After applying the local averaging operator $\mathcal{K}$,

$$\mathcal{K}u_{tt}^\varepsilon - \mathcal{K}(\partial_x A^\varepsilon u_x^\varepsilon) = 0, \tag{4.8}$$

and by using the commutation property on $\partial_t \mathcal{K} = \mathcal{K}\partial_t$ and $\partial_x \mathcal{K} = \mathcal{K}\partial_x$, we arrive at

$$\partial_{tt}(\mathcal{K}u^\varepsilon) - \partial_x(\mathcal{K}A^\varepsilon u_x^\varepsilon) = 0. \tag{4.9}$$

Thus, the PDE we seek for u is of the form,

$$\begin{cases} u_{tt} - \partial_x F = 0, \quad F = \mathcal{K}A^\varepsilon u_x^\varepsilon, \qquad \Omega \times [0, T^\varepsilon], \\ u(x,0) = (\mathcal{K}u^\varepsilon)(x,0), \quad u_t(x,0) = \partial_t(\mathcal{K}u^\varepsilon)(x,0), \qquad \forall x \in \Omega, \end{cases} \tag{4.10}$$

and where u is Ω-periodic in x. A problem that arises in (4.10) is the initial conditions. Assume we have $u^\varepsilon(x,0) = x^3$. Then it turns out that $(\mathcal{K}u^\varepsilon)(x,0)$ is *not* equal to x^3. We have to make a correction to the initial data to make it consistent with the initial data of u^ε. We will discuss this *consistency* condition below in Section 4.2.

Remark 12. *There is no need to consider $v_t \neq 0$ in the micro problem. Take the wave propagation problem of the form*

$$\begin{cases} v_{tt}^\varepsilon - \partial_x(A^\varepsilon v_x^\varepsilon) = 0, \qquad Y^\varepsilon \times [-\tau, \tau], \\ v^\varepsilon(x,0) = v_0(x), \quad v_t^\varepsilon(x,0) = v_1(x), \qquad \forall x \in Y^\varepsilon, \end{cases} \tag{4.11}$$

with periodic boundary conditions in Y^ε. We can split the initial conditions

$$v^\varepsilon(x,0) = v_0(x), \qquad \partial_t v^\varepsilon(x,0) = v_1(x) \tag{4.12}$$

into two parts $v^\varepsilon = v_1^\varepsilon + v_2^\varepsilon$ where v_1^ε solves (4.11) with the initial conditions

$$v_1^\varepsilon(x) = v_0(x), \quad \partial_t v_1^\varepsilon(x,0) = 0, \tag{4.13}$$

and v_2^ε solves (4.11) with the initial conditions

$$v_2^\varepsilon(x) = 0, \quad \partial_t v_2^\varepsilon(x,0) = v_1(x). \tag{4.14}$$

The solution v_1^ε will be time symmetric, i.e., $v_1^\varepsilon(-t, x) = v_1^\varepsilon(t, x)$, and the solution v_2^ε will be anti-symmetric in time, i.e., $v_2^\varepsilon(-t, x) = -v_2^\varepsilon(t, x)$. Let $\mathcal{K}$ be defined as the local averaging operator in Section 2.7, $(\mathcal{K}u)(0,0) = \iint K_\eta K_\tau u \, dt \, dx$. We have,

$$\mathcal{K}v^\varepsilon = \mathcal{K}(v_1^\varepsilon + v_2^\varepsilon) = \mathcal{K}v_1^\varepsilon + \mathcal{K}v_2^\varepsilon = \mathcal{K}v_1^\varepsilon, \tag{4.15}$$

since the mean value of v_2^ε over $-\tau \leq t \leq \tau$ will be zero. With the same argument we know that the mean value of $f^\varepsilon = A^\varepsilon v_x^\varepsilon$ will be independent of the initial data $v_t^\varepsilon(x,0)$. Therefore we need only to consider $v_t^\varepsilon(x,0) = 0$.

Remark 13. *We use the same numerical scheme* (3.3) *to solve the micro problem* (3.4), *with a uniform discretization k in time and h in space,*

$$v_m^{n+1} = 2v_m^n - v_m^{n-1} + \frac{k^2}{24h}\left[-f_{m+\frac{3}{2}}^n + 27f_{m+\frac{1}{2}}^n - 27f_{m-\frac{1}{2}}^n + f_{m-\frac{3}{2}}^n \right] \qquad (4.16)$$

where $f_{m-\frac{1}{2}}^n$ is computed as,

$$f_{m-\frac{1}{2}}^n = \frac{A^\varepsilon\left(x_{m-\frac{1}{2}} + x'\right)}{24h}\left[-v_{m+1}^n + 27v_m^n - 27v_{m-1}^n + v_{m-2}^n \right]. \qquad (4.17)$$

Remark 14. *The weighted integrals in Section 4.1 are computed numerically with a trapezoidal rule in time and a midpoint rule in space which features spectral accuracy for integrals of periodic and compact functions. This is a well known result widely used and at the basis of several integration techniques such as those described in [42].*

Remark 15. *We can reduce the computational cost of the HMM process even further if the function $\tilde{F}$ in* (4.7) *is linear in some of its arguments. We can then apply the HMM process to a smaller number of micro problems and form linear combinations of those for any given $\tilde{F}$ computation. If $\tilde{F}$ depends on u or t it might not be beneficial to precompute $\tilde{F}$ this way. See [24] for further details.*

4.2   Elements of the Method

Now we will describe three important factors in the HMM method: 1) Consistency, in the sense of HMM: between macroscopic solution, reconstruction operator, micro problem and compression operator. 2) Convergence of the macroscopic scheme. 3) Stability of the macroscopic scheme.

Consistency of the Micro Problem

An important aspect in our HMM method is that the initial data for the micro problem is consistent with the current macroscopic state. In practice we approximate the macroscopic state with a third order polynomial $U(x)$ which interpolate the macroscopic grid values $u_{m-2}^n, \ldots, u_{m+1}^n$ in $x_{m-2}, \ldots, x_{m+1}$. We should then choose a polynomial $Q(x)$ as initial data to (3.4) such that

$$U(x) = (\mathcal{K}v^\varepsilon)(0, x). \qquad (4.18)$$

To simplify the discussion we introduce the operator $\mathcal{M}$ which maps the initial data of (3.4) to $(\mathcal{K}v^\varepsilon)(0, x)$. We hence seek Q such that

$$U(x) = (\mathcal{M}Q)(x). \qquad (4.19)$$

We will not be able to find a Q where this is satisfied exactly. However, in this section we will show how to find Q given U such that this equality is satisfied to high order in ε.

When the coefficient $A^\varepsilon(x) = A(x/\varepsilon)$ and $A(y)$ is 1-periodic and Q is a third order polynomial, we showed in [22] that,

$$(\mathcal{M}Q)(x) = Q(x) + \varepsilon^2 \gamma Q''(x) + \mathcal{O}(\varepsilon^3), \tag{4.20}$$

where γ is a constant depending on A. Hence, if we take $Q = U$ we make a $O(\varepsilon^2)$ error. For the long time problem we will need better accuracy. If we know γ we can for instance take

$$Q(x) = U(x) - \varepsilon^2 \gamma U''(x), \tag{4.21}$$

and get an error less than $O(\varepsilon^3)$ in this simple case.

In the general case we will use the following procedure to correct the initial data. We assume that $Q(x) = c_0 + c_1 x + c_2 x^2 + c_3 x^3$ and make that ansatz that

$$(\mathcal{M}Q)(x) \simeq U(x) := \tilde{c}_0 + \tilde{c}_1 x + \tilde{c}_2 x^2 + \tilde{c}_3 x^3. \tag{4.22}$$

Let $\boldsymbol{c}^T = \begin{bmatrix} c_0 & c_1 & c_2 & c_3 \end{bmatrix}$, $\tilde{\boldsymbol{c}}^T = \begin{bmatrix} \tilde{c}_0 & \tilde{c}_1 & \tilde{c}_2 & \tilde{c}_3 \end{bmatrix}$ and $\boldsymbol{x}^T = \begin{bmatrix} 1 & x & x^2 & x^3 \end{bmatrix}$. Then $Q(x) = \boldsymbol{x}^T \boldsymbol{c}$ and $U(x) = \boldsymbol{x}^T \tilde{\boldsymbol{c}}$. Since $\mathcal{M}$ is a linear operator we can represent it by a matrix M acting between the coefficients $\boldsymbol{c}$ and $\tilde{\boldsymbol{c}}$,

$$\tilde{\boldsymbol{c}} = M\boldsymbol{c}. \tag{4.23}$$

The *correction matrix* M can be computed by solving four micro problems with initial data x^j for $j = 0, \ldots, 3$ (details can be found in [22]). With M we can solve (4.23) to obtain $\boldsymbol{c}$ from $\tilde{\boldsymbol{c}}$. We can then also compute the correct flux, without solving more micro problems. For each of the four problems solved we record the corresponding flux and denote it by f_i. Moreover, we set

$$\boldsymbol{f}^T = \begin{bmatrix} f_0 & f_1 & f_2 & f_3 \end{bmatrix}. \tag{4.24}$$

Since the flux computation is also linear in the input $\boldsymbol{c}$ the computed flux from $Q(x)$ is simply

$$F(Q) = \boldsymbol{f}^T \boldsymbol{c}, \tag{4.25}$$

and given $U = \boldsymbol{x}^T \tilde{\boldsymbol{c}}$, the corrected flux is

$$\tilde{F}(U) = \tilde{\boldsymbol{f}}^T \tilde{\boldsymbol{c}}, \qquad \tilde{\boldsymbol{f}} := M^{-T} \boldsymbol{f}. \tag{4.26}$$

For the case when $A^\varepsilon = A(x/\varepsilon)$ and $A(y)$ is periodic we showed in [22] that the correction in Q is precisely what is needed to make the corresponding corrected flux $\tilde{F}$ agree with the flux of the effective equation. With some extra assumptions, Theorem 3 and Theorem 4 in [22] shows that the uncorrected HMM flux is

$$F(U) = \bar{A}U_x + \beta \varepsilon^2 U_{xxx} - \varepsilon^2 \gamma \bar{A} U_{xxx} + O(\alpha^q), \tag{4.27}$$

where γ is the same constant as in (4.20) and $\alpha = \varepsilon/\eta$. The corrected flux, on the other hand, is shown to be

$$\tilde{F}(U) = \bar{A}U_x + \beta\varepsilon^2 U_{xxx} + O(\alpha^q), \tag{4.28}$$

which tends to the flux for the effective equation when the microbox size η gets large in comparison to ε, hence when $\alpha \to 0$.

In Algorithm 4.1 we show an condensed algorithm description how the correction matrices is computed.

Convergence of the Macro Scheme

We proved in [24] that if we apply the HMM to the problem (4.1) with $A^\varepsilon(x) = A(x/\varepsilon)$ where A is a Y-periodic symmetric positive matrix the HMM generates results close to a direct discretization of the homogenized equation (2.12). In particular, we showed that for $Q(x) = \sigma(x - x')$,

$$\tilde{F}(x', Q) = F(x', Q) + \mathcal{O}\left(\left(\frac{\varepsilon}{\eta}\right)^q\right). \tag{4.29}$$

The function $\tilde{F}$ and F are defined in (3.7) and (3.2) respectively and we note that here $F(x', Q) = \bar{A}Q'(x') = \bar{A}\sigma$. The integer q depends on the smoothness of the kernel used to compute the weighted average of f^ε in (3.7).

Theorem 16. *Let $\tilde{F}(x', Q)$ be defined by (3.7) where $Q(x) = \sigma(x - x')$; v^ε solves the micro problem (3.4) exactly; $A^\varepsilon(x) = A(x/\varepsilon)$ and A is Y-periodic and C^∞. Moreover suppose $K \in \mathbb{K}^{p,q}$, f and g are C^∞ and $\tau = \eta$. Then for $\sigma \neq 0$ and any dimension,*

$$\frac{1}{|\sigma|}\left|\tilde{F}(x', Q) - F(x', Q)\right| \leq C\left(\frac{\varepsilon}{\eta}\right)^q, \tag{4.30}$$

where C is independent of ε, η, p and q. Furthermore, for the numerical approximation given in (3.3) in one dimension, with $H = n\varepsilon$ for some integer n and smooth initial data, we have the error estimate

$$|U_m^n - \bar{u}(x_m, t_n)| \leq C(T)\left(H^2 + (\varepsilon/\eta)^q\right), \qquad 0 \leq t_n \leq T, \tag{4.31}$$

where $\bar{u}$ is the homogenized solution to (2.12).

Stability Analysis the Macro Scheme and Regularization

The stability of the long time effective equation (2.52) is a concern, since it is in fact ill-posed. Thus, perturbations in the exact solution grows exponentially in time. Since our HMM algorithm effectively discretizes (2.52) one must be concerned with the stability of the method. In this section we show that as long as the macroscopic discretization is coarse enough, it is indeed stable.

Even though (2.52) is ill-posed, it can be used as an effective equation after regularization. Since we are interested in low frequency solutions it should be possible to use a regularized version of (2.52) where high frequencies are suppressed. The equation could for instance be regularized with a low-pass filter P_{low} applied at the macro level,

$$\tilde{u}_{tt} = P_{\text{low}} \left(\bar{A} \tilde{u}_{xx} + \beta \varepsilon^2 \tilde{u}_{xxxx} \right), \tag{4.32}$$

or by adding a small 6th order term,

$$\tilde{u}_{tt} = \bar{A} \tilde{u}_{xx} + \beta \varepsilon^2 \tilde{u}_{xxxx} + c \varepsilon^4 \tilde{u}_{xxxxxx}, \tag{4.33}$$

cf. (2.51).

Another regularization technique is to use large time and space grid sizes, which can be seen as a type of low-pass filtering. This is what we do in our HMM. We show here that this approach is stable when the coarse grid size H satisfies a standard CFL condition and in addition $H \geq C\varepsilon$, for some constant C. This explains why our HMM is stable. Moreover, even with a coarse grid the macroscopic solution can be computed accurately. In Figure 4.1 we show an example of a solution obtained through a direct discretization of (2.52) on a coarse grid. The solution agrees very well with a direct numerical simulation of the full wave equation.

We now apply standard von Neumann stability analysis [52] to show stability of the macro scheme for periodic solutions,

$$\begin{cases} u_m^{n+1} = 2u_m^n - u_m^{n-1} + \dfrac{K^2}{24H} \left(-f_{m+3/2}^n + 27f_{m+1/2}^n - 27f_{m-1/2}^n + f_{m-3/2}^n \right), \\ f_m^n = (\bar{A}\partial_x + \beta\varepsilon^2\partial_{xxx})p_m^n(x)\big|_{x=x_m}, \end{cases} \tag{4.34}$$

used in the HMM algorithm for the 1d problem and long time. Here we denote u_m^n as the numerical approximation of $u(x_m, t_n)$ and K is the time step and H is the grid size. The scheme (4.34) is fourth order accurate with respect to K and second order with respect to H. We define the interpolation polynomial $p_{m-1/2}^n$ of degree three over four grid points $u_{m-2}^n, \ldots, u_{m+1}^n$ and assume a uniform grid.

Theorem 17. *The finite difference scheme* (4.34) *applied on the effective equation* (2.52) *with 1-periodic boundary conditions is stable, i.e.,*

$$\sum_j (u_j^n)^2 \leq C(T) \sum_j (u_j^0)^2 \qquad n = 1, 2, \ldots, N, \quad Nk = T, \tag{4.35}$$

for some constant $C(T)$ independent of n, for K and H satisfying

$$\frac{\varepsilon}{H} \leq \sqrt{\frac{7\bar{A}}{24\beta}}, \tag{4.36}$$

and

$$\frac{K}{H} \le \frac{24}{\sqrt{\bar{A}}} \sqrt{h\left(\frac{24\varepsilon^2 \beta}{H^2 \bar{A}}\right)}, \tag{4.37}$$

where

$$h(x) = \begin{cases} \dfrac{1}{784 - 112x}, & 0 \le x < \dfrac{21}{5}, \\[2mm] \dfrac{x^2 - 2x + 1}{128\left(2(x^2 - x + 1)^{3/2} - 2x^3 + 3x^2 + 3x - 2\right)}, & \dfrac{21}{5} \le x \le 7. \end{cases} \tag{4.38}$$

The proof is found in [23].

Remark 18. *Recently another effective equation which is also valid up to $T^\varepsilon = \mathcal{O}(\varepsilon^{-2})$ was discovered, [38]. The new equation is well-posed and of the form,*

$$u_{tt} - \bar{A}u_{xx} - \varepsilon^2 \frac{\beta}{\bar{A}} u_{xxtt} = 0, \qquad Y \times [0, T^\varepsilon], \tag{4.39}$$

and with the same initial data as in (2.52). The scalars $\bar{A}$ and β are functions of $A(y)$ over one period. This effective equation, (4.39), is still in flux form as before, $u_{tt} - \partial_x F = 0$, where

$$F = \bar{A}u_x + \varepsilon^2 \frac{\beta}{\bar{A}} u_{xtt}, \tag{4.40}$$

and where F now depends on on partial derivatives of u in t and x. The theory is for $A^\varepsilon(x) = A(x/\varepsilon)$ where $A(y)$ is 1-periodic in y. The same as in the theory by Santosa and Symes [49].

Conclusions

We arrive at three conclusions from the analysis above:

1. The long time effective equation (2.52) is of the form

$$u_{tt} - \partial_x F = 0, \qquad F = \bar{A}u_x + \beta\varepsilon^2 u_{xxx}. \tag{4.41}$$

   This fits into the assumed form of our macroscale PDE in (3.2), $u_{tt} - \nabla \cdot F = 0$, as in Section 2.4, and we do not need to change the HMM algorithm to reflect a different macro model which incorporates dispersive effects.

2. The flux F contains a third derivative of the macroscopic solution. In order to pass this information on to the micro simulation, the initial data must be at least a third order polynomial. This explains why the linear initial data used in the finite time HMM is not enough.

3. Since we need to accurately represent also the second term in the flux F, the error in the flux computation must be smaller than $O(\varepsilon^2)$. The error term for F in Theorem 16 is of the form $(\varepsilon/\eta)^q$. We thus need to chose q and η such that $(\varepsilon/\eta)^q < \varepsilon^2$, or $\eta > \varepsilon^{1-\alpha}$ with $\alpha = 2/q$. Recalling that in the finite time case we always take $\eta \sim \varepsilon$, this hence explains why we need to have more accurate kernels or bigger micro boxes in the long time case. We note that in order to maintain a low computational cost we should have α small, which can be obtained by taking a large q, i.e., a very regular kernel.

Algorithm 4.1 Precomputation of correction matrices $A^{(m)}$, $1 \leq m \leq M$ for the HMM method for long time.

---

for $m = 1 \to M$ **do**
  $x' \leftarrow x_{m-\frac{1}{2}}$
  for $i = 1 \to 4$ **do**
    Initial data $Q(x) \leftarrow x^{i-1}$, i.e., $c_i = 1$ and other $c_j = 0$
    Solve micro problem (3.4) u^ε for all $(x,t) \in [-\eta, \eta] \times [-\tau, \tau]$
    Compute $Y_k \leftarrow \mathcal{K}(u^\varepsilon)(\Delta_k, 0)$ for some distinct Δ_k around $x = 0$
    Find a third degree polynomial that fits (Δ_k, Y_k), which gives $\tilde{c}$.
    $A^{(m)}_{ij} = \tilde{c}_{j-1}, \quad 1 \leq j \leq 4$
  end for
end for

Algorithm 4.2 HMM algorithm for the long time wave equation. Uses microsolver Algorithm 4.3

Discretize domain Ω into $x_0, x_1, \ldots, x_m \in \Omega$ and time $[0, T^\varepsilon]$ into $t_0, t_1, \ldots, t_N$ such that the grid x_k is aligned with the macro grid, and the initial data is resolved, and $\lambda = \frac{\Delta t}{\Delta x}$ satisfies the CFL condition $a_{\max} \frac{\Delta t}{\Delta x} \leq 1$.
Compute initial data $u_m^0 = u_0(x_m)$ and $u_m^{-1} = u_0(x_m) + \frac{k^2}{24h}\left[-f^n_{m+\frac{3}{2}} + 27f^n_{m+\frac{1}{2}} - 27f^n_{m-\frac{1}{2}} + f^n_{m-\frac{3}{2}}\right]$.
OPTIONAL: Precompute fluxes
for $n = 0, 1, \ldots, M$ **do**
  Precompute fluxes as described in Algorithm 4.1 including the correction
end for
MAIN LOOP: Time step solution
for $n = 0, 1, \ldots, N$ **do**
  Update u_m^{n+1} as in (4.5).
end for
IMPORTANT: If the precomputation step is ignored the correction is still needed in each grid point, each time step.

.

Algorithm 4.3 microsolver: Compute $\tilde{F}$ given x' and $Q(x)$.

Pick Y^ε such that $Y^\varepsilon = [-y_{\max}, y_{\max}]$ and $y_{\max} = \eta + \tau \max_{x \in Y^\varepsilon} \sqrt{A^\varepsilon(x)}$.

Discretize Y^ε into $x_0, x_1, \ldots, x_M$ and time $[-\tau, \tau]$ into $t_0, t_1, \ldots, t_N$ such that $\frac{\varepsilon}{\Delta x} = \rho$ (points per wave length measure) and $\lambda = \frac{\Delta t}{\Delta x}$ satisfies the CFL condition $a_{\max} \frac{\Delta t}{\Delta x} \leq 1$.

Compute initial data $(v^\varepsilon)^0_m = Q(x_m)$ and $(v^\varepsilon)^{-1}_m = v^n_m - \frac{\Delta t^2}{2} D^+ F^0_m$ where F is the numerical flux (4.17) and D^+ is a forth order discretization of ∂_x.

for $n = 0, 1, \ldots, N$ **do**

    Compute v^{n+1}_m according to Remark 13.

    Compute $G^n = \Delta x \sum_{m=0}^{M} K_\eta(x_m) v^n_m$.

end for

Compute $\tilde{F} = \Delta t \sum_{n=-N}^{N} \mathcal{K}_\tau(t_n) G^n$ where $t^{-n} = t^n$ and $G^{-n} = G^n$.

4.3 Numerical Results

We present a final comparison based on the the wave equation (4.3) with the following parameters

$$
\begin{cases}
A^\varepsilon(x) = 1.1 + \sin \dfrac{2\pi x}{\varepsilon}, \\
\bar{A} = \sqrt{0.21}, \quad \beta \approx 0.01078280318, \\
\Omega = [0, 1], \quad T = 100 \times \sqrt{\bar{A}}
\end{cases}
\tag{4.42}
$$

in Figure 4.1. For the micro problem we use 128 points per ε. The homogenized and effective equation uses roughly 350 points for the discretization of $\Omega = [0, 1]$, as many grid points as the stability allows us, cf. Section 4.2. See Figure 4.1 for a plot of the three solutions: the exact, HMM and the solution of the effective equation (EFF).
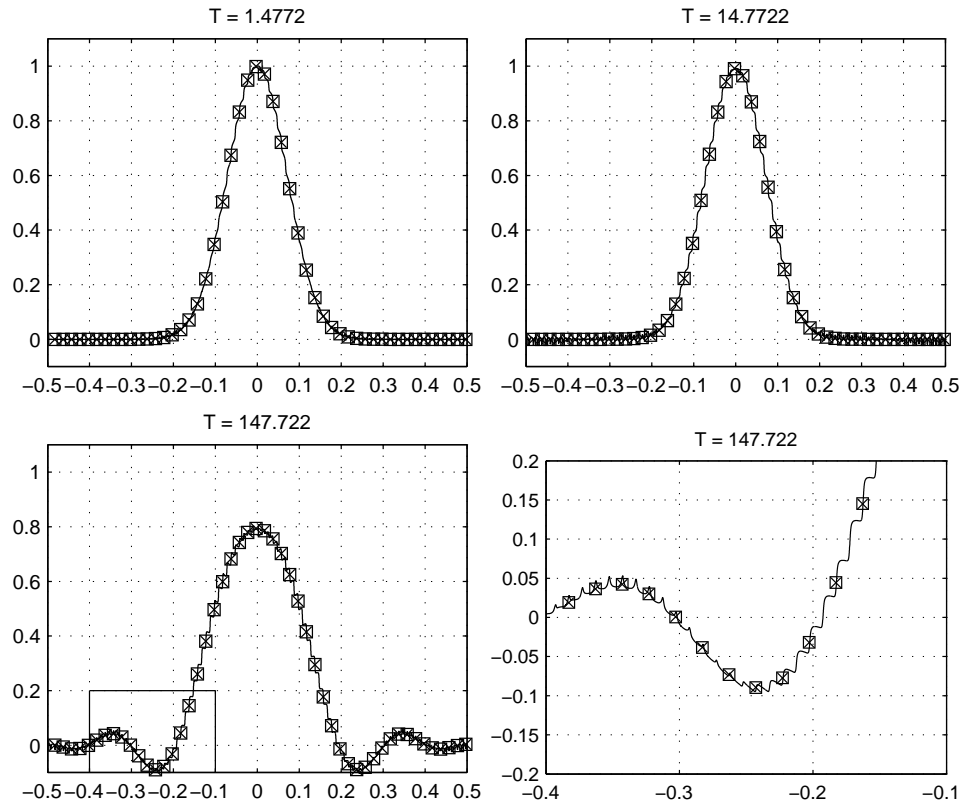
Figure 4.1: Numerical result from a long time DNS computation (thin line) compared to a direct discretization of the long time effective equation (2.52) with a coarse grid (squares) and our HMM method (crosses).

Chapter 5

Summary of Paper V: HMM for High Frequency Initial Data in One Dimension

In this paper we consider the following form of the multiscale wave equation (2.10), in one dimension,

$$\begin{cases} u_{tt}^\varepsilon - \partial_x(a^2 u^\varepsilon) = 0, & \Omega \times [0, T], \\ u^\varepsilon(x, 0) = u_0^\varepsilon(x), \quad u_t^\varepsilon(x, 0) = u_1^\varepsilon(x), & \forall x \in \Omega, \end{cases} \tag{5.1}$$

where u^ε is Ω-periodic.

Our HMM method for this problem [25] uses ideas from geometrical optics, deals with non-oscillating $a^2(x)$ which is scalar, uniformly positive and Ω-periodic; finite $T = \mathcal{O}(1)$; and where the initial data is oscillating with frequencies of order ε^{-1}. In Section 2.6 we described how u^ε can be approximated by $u^\varepsilon \approx \exp(i\phi(x, t)/\varepsilon)A(x, t)$ where the phase ϕ and amplitude A are slowly varying functions of x,

$$\begin{cases} \phi_t + c|\nabla\phi| = 0, \\ (A_0)_t + \dfrac{\nabla\phi \cdot \nabla A_0}{|\nabla\phi|} + \dfrac{c^2\nabla^2\phi - \phi_{tt}}{2c|\nabla\phi|} = 0, \\ \phi(x, 0) = \dfrac{\varepsilon}{i} \log \dfrac{u^\varepsilon(x, 0)}{|u^\varepsilon(x, 0)|}, \quad A(x, 0) = |u_0(x, 0)|^2, \end{cases} \tag{5.2}$$

where the equation above describes a right going wave. Usually the direction of the wave is determined by the initial conditions of the wave equation. It can also be a bi-directional wave going both left and right on the real line.

Geometrical optics and asymptotic expansions of the solution u^ε to (5.1) have given rise to many other numerical methods for highly oscillatory problems. Among the more famous ones we have: ray tracing [6, 28] where the system is formulated as a system of ODEs describing the phase and amplitude; and wavefront methods [28].

The geometrical optics approach has been generalized in many directions. Since there exists mathematical challenges in the GO model (e.g., caustics and focus of rays) other mathematical models have been suggested. For instance a kinetic model [28]; the segment projection method [29]; and Gaussian beams tracing rays containing both amplitude and phase incorporated into one beam [53]. The effect on boundary conditions is included in the geometrical theory of diffraction, [36].

We will demonstrate, by WKB expansions of some quantities of interest, related to the solution u^ε, that right and left going energy is a suitable macroscopic interest since it is slowly varying in the leading terms whereas the amplitude $|u^\varepsilon|$ is oscillatory. Thereafter we describe the HMM method for the energy and the related microproblem. We show an experiment similar to one experiment in [25] which solves a multiscale problem of type A: we have a known macroscopic model almost everywhere in the domain Ω except at two grid-points where a^2 has a jump. In this point we will use HMM micro problems to find out the correct behavior.

5.1 Asymptotic Expansions of Important Quantities

In this section we will consider waves going in both left and right directions. We will show asymptotic expansions for the amplitude; scaled energy E; and the scaled left and right going fluxes F^L and F^R.

Throughout this section we will use the WKB expansion of u^ε for bi-directional wave propagation,

$$u^\varepsilon(x,t) = \mathcal{A}(x,t)e^{i\alpha(x,t)/\varepsilon} + \mathcal{B}(x,t)e^{i\beta(x,t)/\varepsilon}, \tag{5.3}$$

where

$$\mathcal{A}(x,t) = \sum_{k=0}^{\infty} A_k(x,t)(i\varepsilon)^k, \quad \mathcal{B}(x,t) = \sum_{k=0}^{\infty} B_k(x,t)(i\varepsilon)^k, \tag{5.4}$$

and α and A_k solves the $+$ version and β and B_k solves the $-$ version of (2.69). Hence,

$$\begin{cases} \alpha_t + a\alpha_x = 0, \\ \beta_t - a\beta_x = 0. \end{cases} \tag{5.5}$$

The phases α and β thus correspond to right and left going waves, respectively. We use the notation z^* for the complex conjugate of z and all integrals are taken over $\mathbb{R}$ unless it is explicitly given.

Amplitude

In this section we want to describe the leading terms proportional to $1, \varepsilon$ and ε^2 of the square amplitude of the solution u^ε to (5.1). By using the WKB expansion

(5.3) we have,

$$
\begin{aligned}
|u^\varepsilon|^2 =& |\mathcal{A}|^2 + |\mathcal{B}|^2 + 2\Re\left\{\mathcal{A}\mathcal{B}^* e^{i(\alpha-\beta)/\varepsilon}\right\} \\
=& |A_0 + i\varepsilon A_1 + \mathcal{O}(\varepsilon^2)|^2 + |B_0 + i\varepsilon B_1 + \mathcal{O}(\varepsilon^2)|^2 + 2\Re\left\{\mathcal{A}\mathcal{B}^* e^{i(\alpha-\beta)/\varepsilon}\right\}.
\end{aligned}
\tag{5.6}
$$

We use the fact that,

$$
\begin{aligned}
\Re\left\{\mathcal{A}\mathcal{B}^* e^{i(\alpha-\beta)/\varepsilon}\right\} &= \Re\left\{\left(A_0 B_0 + i\varepsilon A_1 B_0 - i\varepsilon A_0 B_1 + \mathcal{O}(\varepsilon^2)\right) e^{i(\alpha-\beta)/\varepsilon}\right\} \\
&= A_0 B_0 \cos\frac{\alpha-\beta}{\varepsilon} + \varepsilon(A_0 B_1 - A_1 B_0)\sin\frac{\alpha-\beta}{\varepsilon} + \mathcal{O}(\varepsilon^2), \quad (5.7)
\end{aligned}
$$

which gives us the result we are looking for,

$$
\begin{aligned}
|u^\varepsilon|^2 =& A_0^2 + B_0^2 + 2A_0 B_0 \cos\frac{\alpha-\beta}{\varepsilon} + \\
& 2\varepsilon(A_0 B_1 - A_1 B_0)\sin\frac{\alpha-\beta}{\varepsilon} + \mathcal{O}(\varepsilon^2).
\end{aligned}
\tag{5.8}
$$

The $\mathcal{O}(\varepsilon^2)$ term in (5.8) will contain both oscillatory and slowly varying terms. The $\mathcal{O}(1)$ and $\mathcal{O}(\varepsilon)$ terms are both oscillatory. The $\mathcal{O}(1)$ terms have mean value $A_0^2 + B_0^2$ and the $\mathcal{O}(\varepsilon)$ terms have mean value zero.

Energy

We define the scaled pointwise energy $E(x,t)$ for the solution u^ε to (5.1) as,

$$
E(x,t) = \frac{\varepsilon^2}{2}|u_t^\varepsilon(x,t)|^2 + \frac{\varepsilon^2 a^2(x)}{2}|u_x^\varepsilon(x,t)|^2.
\tag{5.9}
$$

In this section we will compute the asymptotic expansion of E. For that we need to compute the asymptotics of both $|u_t^\varepsilon|^2$ and $|u_x^\varepsilon|^2$. We have for $|u_t^\varepsilon|^2$,

$$
\begin{aligned}
|u_t^\varepsilon|^2 =& \left|\left(\frac{i\alpha_t}{\varepsilon}\mathcal{A} + \mathcal{A}_t\right)e^{i\frac{\alpha}{\varepsilon}} + \left(\frac{i\beta_t}{\varepsilon}\mathcal{B} + \mathcal{B}_t\right)e^{i\frac{\beta}{\varepsilon}}\right|^2 \\
=& \left|\frac{i\alpha_t}{\varepsilon}\mathcal{A} + \mathcal{A}_t\right|^2 + \left|\frac{i\beta_t}{\varepsilon}\mathcal{B} + \mathcal{B}_t\right|^2 + 2\Re\left\{\left(\frac{i\alpha_t}{\varepsilon}\mathcal{A} + \mathcal{A}_t\right)\overline{\left(\frac{i\beta_t}{\varepsilon}\mathcal{B} + \mathcal{B}_t\right)}e^{i\frac{\alpha-\beta}{\varepsilon}}\right\} \\
=& \left|\frac{i\alpha_t}{\varepsilon}\left(A_0 + i\varepsilon A_1 - \varepsilon^2 A_2 + \mathcal{O}(\varepsilon^3)\right) + (A_0)_t + i\varepsilon(A_1)_t + \mathcal{O}(\varepsilon^2)\right|^2 \\
& + \left|\frac{i\beta_t}{\varepsilon}\left(B_0 + i\varepsilon B_1 - \varepsilon^2 B_2 + \mathcal{O}(\varepsilon^3)\right) + (B_0)_t + i\varepsilon(B_1)_t + \mathcal{O}(\varepsilon^2)\right|^2 \\
& + 2\Re\left\{\left(\frac{i\alpha_t}{\varepsilon}\mathcal{A} + \mathcal{A}_t\right)\overline{\left(\frac{i\beta_t}{\varepsilon}\mathcal{B} + \mathcal{B}_t\right)}e^{i\frac{\alpha-\beta}{\varepsilon}}\right\}.
\end{aligned}
\tag{5.10}
$$

We now consider only the first term in the above expression,

$$\left| \frac{i\alpha_t}{\varepsilon}\left(A_0 + i\varepsilon A_1 - \varepsilon^2 A_2 + \mathcal{O}(\varepsilon^3)\right) + (A_0)_t + i\varepsilon(A_1)_t + \mathcal{O}(\varepsilon^2)\right|^2$$

$$= \left| \frac{i\alpha_t}{\varepsilon}A_0 - \alpha_t A_1 - i\varepsilon\alpha_t A_2 + (A_0)_t + i\varepsilon(A_1)_t + \mathcal{O}(\varepsilon^2)\right|^2$$

$$= \left| i\left(\frac{\alpha_t}{\varepsilon}A_0 + \varepsilon(-\alpha_t A_2 + (A_1)_t)\right) - \alpha_t A_1 + (A_0)_t\right|^2 + \mathcal{O}(\varepsilon^2) \qquad (5.11)$$

$$= \left| \frac{\alpha_t}{\varepsilon}A_0 + \varepsilon(-\alpha_t A_2 + (A_1)_t)\right|^2 + \left| -\alpha_t A_1 + (A_0)_t\right|^2 + \mathcal{O}(\varepsilon^2)$$

$$= \frac{\alpha_t^2}{\varepsilon^2}A_0^2 + 2\alpha_t A_0(-\alpha_t A_2 + (A_1)_t) + (-\alpha_t A_1 + (A_0)_t)^2 + \mathcal{O}(\varepsilon^2).$$

The second term is on the same form,

$$\frac{\beta_t^2 B_0^2}{\varepsilon^2} + 2\beta_t B_0(-\beta_t B_2 + (B_1)_t) + (-\beta_t B_1 + (B_0)_t)^2 + \mathcal{O}(\varepsilon^2). \qquad (5.12)$$

The last term is expressed as,

$$2\Re\left\{\left(\frac{i\alpha_t}{\varepsilon}\mathcal{A} + \mathcal{A}_t\right)\overline{\left(\frac{i\beta_t}{\varepsilon}\mathcal{B} + \mathcal{B}_t\right)}e^{i\frac{\alpha-\beta}{\varepsilon}}\right\} =$$

$$2\Re\left\{\left(\frac{\alpha_t\beta_t}{\varepsilon^2}\mathcal{A}\mathcal{B}^* + \mathcal{A}_t\mathcal{B}_t^* + \frac{i(\alpha_t\mathcal{A}\mathcal{B}_t^* - \beta_t\mathcal{A}_t\mathcal{B}^*)}{\varepsilon}\right)e^{i\frac{\alpha-\beta}{\varepsilon}}\right\}. \qquad (5.13)$$

After a similar calculation for $a^2|u_x^\varepsilon|^2$ we obtain

$$E = \tfrac{1}{2}\alpha_t^2 A_0^2 + \tfrac{1}{2}\beta_t^2 B_0^2 + \tfrac{1}{2}a^2\alpha_x^2 A_0^2 + \tfrac{1}{2}a^2\beta_x^2 B_0^2 + \mathcal{O}(\varepsilon^2)$$

$$+ \Re\left\{\left(\alpha_t\beta_t + a^2\alpha_x\beta_x\right)\mathcal{A}\mathcal{B}^* + i\varepsilon((\alpha_t + a^2\alpha_x)\mathcal{A}\mathcal{B}_t^* - (\beta_t + a^2\beta_x)\mathcal{A}_t\mathcal{B}^*)e^{i\frac{\alpha-\beta}{\varepsilon}}\right\}. \qquad (5.14)$$

By using the fact that α_t and β_t solve (5.5) we have, $\alpha_t\beta_t = -a^2\alpha_x\beta_x$. Hence,

$$E = a^2\alpha_x^2 A_0^2 + a^2\beta_x^2 B_0^2 - \varepsilon\sin(\tfrac{\alpha-\beta}{\varepsilon})\Big(\alpha_t A_0(B_0)_t - \beta_t(A_0)_t B_0$$

$$+ a^2\alpha_x A_0(B_0)_x - a^2\beta_x(A_0)_x B_0\Big)$$

$$+ \mathcal{O}(\varepsilon^2). \qquad (5.15)$$

When α and β are matched with a this simplifies to

$$E = A_0^2 + B_0^2 - \varepsilon\sin(\tfrac{\alpha-\beta}{\varepsilon})\Big(\alpha_t A_0(B_0^*)_t - \beta_t(A_0)_t B_0$$

$$+ a^2\alpha_x A_0(B_0)_x - a^2\beta_x(A_0)_x B_0\Big) + \mathcal{O}(\varepsilon^2). \qquad (5.16)$$

The $\mathcal{O}(1)$ part in the WKB expansion (5.15) is non-oscillatory and the $\mathcal{O}(\varepsilon)$ and $\mathcal{O}(\varepsilon^2)$ part is oscillatory.

Flux

In this section we will derive an advection equation corresponding to the scaled energy E of the solution to (5.1). We will also compute asymptotic expansions for the involved quantities. To derive the advection equation we note that,

$$\partial_t |z|^2 = \partial_t(zz^*) = z_t z^* + z z_t^* = 2\Re(zz_t^*). \tag{5.17}$$

Therefore we can express the time derivate E_t as

$$\frac{1}{\varepsilon^2} E_t = \Re(u_t^\varepsilon (u_{tt}^\varepsilon)^*) + a^2 \Re(u_x^\varepsilon (u_{xt}^\varepsilon)^*) \tag{5.18}$$

$$= \Re(u_t^\varepsilon \partial_x(a^2(u_x^\varepsilon)^*) + a^2 u_x^\varepsilon (u_{xt}^\varepsilon)^*) \tag{5.19}$$

$$= \Re((u_t^\varepsilon)^* \partial_x(a^2 u_x^\varepsilon) + a^2 u_x^\varepsilon (u_{xt}^\varepsilon)^*) \tag{5.20}$$

$$= \Re(\partial_x\left((u_t^\varepsilon)^* a^2 u_x^\varepsilon\right)), \tag{5.21}$$

$$= \partial_x\left[a^2 \Re((u_t^\varepsilon)^* u_x^\varepsilon)\right]. \tag{5.22}$$

This shows that the advection equation for the energy is in conservative form,

$$E_t = \partial_x F, \tag{5.23}$$

where the flux F is of the form,

$$F = a^2 \varepsilon^2 \Re((u_t^\varepsilon)^* u_x^\varepsilon). \tag{5.24}$$

Furthermore, we define the right- and left going fluxes F^R and F^L by

$$F^R = -\frac{a\varepsilon^2}{4}|u_t^\varepsilon - au_x^\varepsilon|^2, \qquad F^L = \frac{a\varepsilon^2}{4}|u_t^\varepsilon + au_x^\varepsilon|^2, \tag{5.25}$$

where we note that,

$$F^L + F^R = \frac{a\varepsilon^2}{4}\left(|u_t^\varepsilon + au_x^\varepsilon|^2 - |u_t^\varepsilon - au_x^\varepsilon|^2\right) \tag{5.26}$$

$$= \frac{a\varepsilon^2}{4}\left(|u_t^\varepsilon|^2 + 2\Re(au_t^\varepsilon(u_x^\varepsilon)^*) + a^2|u_x^\varepsilon|^2 - |u_t^\varepsilon|^2 + 2\Re(au_t^\varepsilon(u_x^\varepsilon)^*) - a^2|u_x^\varepsilon|^2\right),$$
$$\tag{5.27}$$

$$= \varepsilon^2 a^2 \Re((u^\varepsilon)_t^* u_x^\varepsilon), \tag{5.28}$$

which is the same flux as we defined in (5.24), hence $F = F^R + F^L$.

We give a motivation to the notation right- and left-going energy flux in the following way: Suppose a is approximately constant in a $\mathcal{O}(\varepsilon)$ neighborhood of x_0. We can then use the d'Alembert solution formula and approximate,

$$u^\varepsilon \approx u^L + u^R, \tag{5.29}$$

where u^R and u^L satisfies $u_t^R + au_x^R = 0$ and $u_t^L - au_x^L = 0$. The fact that,

$$u_t^\varepsilon + au_x^\varepsilon = u_t^R + au_x^R + u_t^L + au_x^L = u_t^L + au_x^L = 2au_x^L = 2u_t^L, \tag{5.30}$$

implies that,

$$F^L = \frac{a\varepsilon^2}{4}|u_t + au_x|^2 = a\varepsilon^2\Re(u_t^L(u_t^L)^*) = a^2\varepsilon^2\Re((u_t^L)^* u_x^L). \tag{5.31}$$

Similarly we have,

$$F^R = -\frac{a\varepsilon^2}{4}|u_t - au_x|^2 = -a\varepsilon^2\Re((u_t^R)^* u_t^R) = a^2\varepsilon^2\Re((u_t^R)^* u_x^R). \tag{5.32}$$

These are thus of the same form as (5.24) but with u^ε replaced by u^L and u^R.

Let us now derive, asymptotic expansions for the these fluxes. We have

$$u_t^\varepsilon = \left(\frac{i\alpha_t}{\varepsilon}\mathcal{A} + \mathcal{A}_t\right)e^{i\alpha/\varepsilon} + \left(\frac{i\beta_t}{\varepsilon}\mathcal{B} + \mathcal{B}_t\right)e^{i\beta/\varepsilon} \tag{5.33}$$

and

$$u_x^\varepsilon = \left(\frac{i\alpha_x}{\varepsilon}\mathcal{A} + \mathcal{A}_x\right)e^{i\alpha/\varepsilon} + \left(\frac{i\beta_x}{\varepsilon}\mathcal{B} + \mathcal{B}_x\right)e^{i\beta/\varepsilon}. \tag{5.34}$$

This shows that

$$u_t^\varepsilon + au_x^\varepsilon = \left(\frac{i(\alpha_t + a\alpha_x)}{\varepsilon}\mathcal{A} + \mathcal{A}_t + a\mathcal{A}_x\right)e^{i\alpha/\varepsilon} + \left(\frac{i(\beta_t + a\beta_x)}{\varepsilon}\mathcal{B} + \mathcal{B}_t + a\mathcal{B}_x\right)e^{i\beta/\varepsilon}. \tag{5.35}$$

We now apply (5.5) and expand in powers of ε,

$$|u_t^\varepsilon + au_x^\varepsilon|^2 = \left|(\mathcal{A}_t + a\mathcal{A}_x)e^{i\alpha/\varepsilon} + \left(\frac{2ia\beta_x}{\varepsilon}\mathcal{B} + \mathcal{B}_t + a\mathcal{B}_x\right)e^{i\beta/\varepsilon}\right|^2 \tag{5.36}$$

$$= |\mathcal{A}_t + a\mathcal{A}_x|^2 + \left|\frac{2ia\beta_x}{\varepsilon}\mathcal{B} + \mathcal{B}_t + a\mathcal{B}_x\right|^2 \tag{5.37}$$

$$+ 2\Re\left\{(\mathcal{A}_t + a\mathcal{A}_x)\left(-\frac{2ia\beta_x}{\varepsilon}\mathcal{B}^* + \mathcal{B}_t^* + a\mathcal{B}_x^*\right)e^{i(\alpha-\beta)/\varepsilon}\right\} \tag{5.38}$$

$$= \mathcal{O}(1) + \left|\frac{2ia\beta_x}{\varepsilon}(B_0 + \mathcal{O}(\varepsilon)) + \mathcal{O}(1)\right|^2 \tag{5.39}$$

$$+ 2\Re\left\{-\frac{2ia\beta_x}{\varepsilon}(B_0 + \mathcal{O}(\varepsilon))((A_0)_t + a(A_0)_x + \mathcal{O}(\varepsilon))e^{i(\alpha-\beta)/\varepsilon}\right\} \tag{5.40}$$

$$= \frac{4a^2\beta_x^2 B_0^2}{\varepsilon^2} + \frac{4a\beta_x}{\varepsilon}B_0((A_0)_t + a(A_0)_x)\sin(\frac{\alpha-\beta}{\varepsilon}) + \mathcal{O}(1). \tag{5.41}$$

A similar calculation for $|u_t^\varepsilon - au_x^\varepsilon|^2$:

$$|u_t^\varepsilon - au_x^\varepsilon|^2 = \left| \left(\frac{-2ia\alpha_x}{\varepsilon} \mathcal{A} + \mathcal{A}_t - a\mathcal{A}_x \right) e^{i\alpha/\varepsilon} + (\mathcal{B}_t - a\mathcal{B}_x) e^{i\beta/\varepsilon} \right|^2 \tag{5.42}$$

$$= \left| \frac{-2ia\alpha_x}{\varepsilon} \mathcal{A} + \mathcal{A}_t - a\mathcal{A}_x \right|^2 + |\mathcal{B}_t - a\mathcal{B}_x|^2 \tag{5.43}$$

$$+ 2\Re \left\{ (\mathcal{B}_t - a\mathcal{B}_x) \left(\frac{2ia\alpha_x}{\varepsilon} \mathcal{A}^* + \mathcal{A}_t^* - a\mathcal{A}_x^* \right) e^{i(\beta - \alpha)/\varepsilon} \right\} \tag{5.44}$$

$$= \mathcal{O}(1) + \left| -\frac{2ia\alpha_x}{\varepsilon} (A_0 + \mathcal{O}(\varepsilon)) + \mathcal{O}(1) \right|^2 \tag{5.45}$$

$$+ 2\Re \left\{ \frac{2ia\alpha_x}{\varepsilon} (A_0 + \mathcal{O}(\varepsilon))((B_0)_t - a(B_0)_x + \mathcal{O}(\varepsilon)) e^{i(\beta - \alpha)/\varepsilon} \right\} \tag{5.46}$$

$$= \frac{4a^2\alpha_x^2 A_0^2}{\varepsilon^2} + \frac{4a\alpha_x}{\varepsilon} A_0((B_0)_t - a(B_0)_x) \sin(\tfrac{\alpha - \beta}{\varepsilon}) + \mathcal{O}(1). \tag{5.47}$$

In conclusion,

$$\begin{cases} F^R = -a^3\alpha_x^2 A_0^2 - \varepsilon a^2\alpha_x A_0((B_0)_t - a(B_0)_x) \sin(\tfrac{\alpha - \beta}{\varepsilon}) + \mathcal{O}(\varepsilon^2), \\ F^L = a^3\beta_x^2 B_0^2 + \varepsilon a^2\beta_x B_0((A_0)_t + a(A_0)_x) \sin(\tfrac{\alpha - \beta}{\varepsilon}) + \mathcal{O}(\varepsilon^2). \end{cases} \tag{5.48}$$

We showed that $F = F^R + F^L$ so the above computations also gives an asymptotic expansion for the scaled flux F, therefore

$$F = a^3 \left(\beta_x^2 B_0^2 - \alpha_x^2 A_0^2 \right)$$
$$+ \varepsilon a^2 \sin(\tfrac{\alpha - \beta}{\varepsilon}) \left(\beta_x B_0((A_0)_t + a(A_0)_x) - \alpha_x A_0((B_0)_t - a(B_0)_x) \right) + \mathcal{O}(\varepsilon^2). \tag{5.49}$$

When α and β are matched with a this simplifies to,

$$\begin{cases} F^R = -aA_0^2 - \varepsilon a^2\alpha_x A_0((B_0)_t + a(B_0)_x) \sin(\tfrac{\alpha - \beta}{\varepsilon}) + \mathcal{O}(\varepsilon^2), \\ F^L = aB_0^2 + \varepsilon a^2\beta_x B_0((A_0)_t + a(A_0)_x) \sin(\tfrac{\alpha - \beta}{\varepsilon}) + \mathcal{O}(\varepsilon^2), \end{cases} \tag{5.50}$$

and

$$F = a \left(B_0^2 - A_0^2 \right)$$
$$+ \varepsilon a^2 \sin(\tfrac{\alpha - \beta}{\varepsilon}) \left(\beta_x B_0((A_0)_t + a(A_0)_x) - \alpha_x A_0((B_0)_t - a(B_0)_x) \right) + \mathcal{O}(\varepsilon^2). \tag{5.51}$$

The $\mathcal{O}(1)$ and $\mathcal{O}(\varepsilon^2)$ terms will be slowly varying as we see clearly from the computations. The terms of order ε are oscillatory with mean value zero.

Local Average and Kernels

For the scaled energy E and the scaled flux F, we arrived at asymptotic expansions of the form,

$$X^\varepsilon = X_0 + \varepsilon \sin\left(\frac{\beta - \alpha}{\varepsilon}\right) f(x,t) + \mathcal{O}(\varepsilon^2), \tag{5.52}$$

where f is a slowly varying function. The second term is thus highly oscillatory. In general these kind of terms are undesirable and problematic from a numerical perspective.

Suppose we want to compute X_0 but only have X^ε. We will be able to do that to $\mathcal{O}(\varepsilon^2)$ accuracy if we could average away the oscillatory part. We suggest that we can reduce the oscillations by instead of taking a point sample of $X^\varepsilon(x,t)$ to approximate $X_0(x,t)$, we compute the average,

$$\bar{X}(x,y) = \frac{1}{4\eta\tau} \int_{x-\eta}^{x+\eta} \int_{t-\tau}^{t+\tau} X^\varepsilon(x+\xi, t+\varphi) \, \mathrm{d}\xi \, \mathrm{d}\varphi, \tag{5.53}$$

for some choice of η and τ depending on the periodicity of the oscillations. This idea can be improved even further by using a smooth kernel,

$$\bar{X}(x,y) = \frac{1}{\tau\eta} \iint K(\tfrac{t}{\tau}) K(\tfrac{x}{\eta}) X^\varepsilon(x+\xi, t+\varphi) \, \mathrm{d}\xi \, \mathrm{d}\varphi =: (\mathcal{K}X^\varepsilon)(x,t), \tag{5.54}$$

denoted here as a local mean value, with a kernel K. We described kernels in Section 2.7. We refer to [24] where we used this technique and [31] for a mathematical description.

To apply Theorem 4 we need to be able to write the oscillatory term on the form $g(x,t,\frac{x}{\varepsilon},\frac{t}{\varepsilon})$. We can for instance take $g(x,t,\xi,\varphi) = \sin(\xi/x)(\alpha(x,t)-\beta(x,t))f(x,t)$, and assuming $\alpha \neq \beta$, we see that g is smooth in all variables. If $\alpha = \beta$ the oscillatory term disappears completely. However, the function g is not 1-periodic in ξ. Nevertheless, we observe the same dependence on η, τ as in Theorem 4 in our numerical experiments, thus we expect it is possible to reduce the difference to,

$$|X_0(x,t) - \bar{X}(x,t)| = \mathcal{O}(\varepsilon(\tfrac{\varepsilon}{\eta})^q) + \mathcal{O}(\varepsilon(\tfrac{\varepsilon}{\tau})^q) + \mathcal{O}(\varepsilon\eta^p) + \mathcal{O}(\varepsilon\tau^p) + \mathcal{O}(\varepsilon^2). \tag{5.55}$$

Note that we can make the difference $|X_0 - X^\varepsilon| = \mathcal{O}(\varepsilon^2)$ by choosing the kernel parameters η, τ, p and q as,

$$\eta, \tau \sim \varepsilon^\gamma, \quad \gamma = \frac{1}{p}, \quad \frac{1}{p} + \frac{1}{q} = 1. \tag{5.56}$$

The same idea can be applied to the square amplitude but we need to use a slightly larger box $\eta, \tau \sim \varepsilon^\gamma$, where $\gamma = \frac{2}{p}$.

We define the quantities,

$$\begin{cases} \bar{E} = \mathcal{K}E, \quad \bar{A} = \mathcal{K}|u^\varepsilon|^2, \\ \bar{F}^R = \mathcal{K}F^R, \quad \bar{F}^L = \mathcal{K}F^L, \end{cases} \tag{5.57}$$

and with the appropriate choices of K, η and τ we have the asymptotic expansions,

$$\begin{cases} \bar{E} = a^2 \alpha_x^2 A_0^2 + a^2 \beta_x^2 B_0^2 + \mathcal{O}(\varepsilon^2), \quad \bar{A} = A_0^2 + B_0^2 + \mathcal{O}(\varepsilon^2), \\ \bar{F}^R = -a^3 \alpha_x^2 A_0^2 + \mathcal{O}(\varepsilon^2), \quad \bar{F}^L = a^3 \beta_x^2 B_0^2 + \mathcal{O}(\varepsilon^2). \end{cases} \tag{5.58}$$

5.2 The Method

In this section we will describe our HMM method for the wave equation (5.1). We will assume that the initial data is of the form,

$$u_0^\varepsilon(x) = A(x) e^{i\phi(x,0)/\varepsilon}, \text{ and either } u_1^\varepsilon(x) = 0 \text{ or } u_1^\varepsilon(x) = -\frac{i}{\varepsilon} u_0^\varepsilon(x), \tag{5.59}$$

where ϕ is matched with a, as in Remark 3. The scaled energy E at $t = 0$ is asymptotically equal to $\frac{1}{2} A^2(x) + \mathcal{O}(\varepsilon^2)$.

We will first assume that the phase is matched with a as described in the end of Section 2.6 in Remark 3. In Chapter 6 we will discuss how this assumption can be avoided.

Macro Model and Discretizeation

We defined the scaled energy E for solutions of (5.1) as the sum of its kinetic energy and potential energy in (5.9) and the local mean energy as $\bar{E} = \mathcal{K}E$ in Section 5.1. It is easy to show that ∂_x and ∂_t commutes with the local mean operator $\mathcal{K}$ defined in (5.54). By applying the mean value operator $\mathcal{K}$ to (5.24) we obtain the following left hand side,

$$\mathcal{K}(E_t) = \partial_t \mathcal{K}E = \bar{E}_t, \tag{5.60}$$

and for the right hand side,

$$\mathcal{K}\partial_x F = \partial_x \mathcal{K}F = \partial_x \bar{F}. \tag{5.61}$$

Thus, we have that

$$\bar{E}_t = \partial_x \bar{F}. \tag{5.62}$$

Inspired by this we choose our macroscopic variables as the local mean right and left going energy $\bar{E}^R$ and $\bar{E}^L$. They should satisfy that $\bar{E} = \bar{E}^R + \bar{E}^L$ and we assume they solve the PDE:

$$\begin{cases} \bar{E}_t^R - \bar{F}_x^R = 0, \quad \Omega \times [0,T], \\ \bar{E}_t^L - \bar{F}_x^L = 0, \quad \Omega \times [0,T], \end{cases} \tag{5.63}$$

with initial data

$$\bar{E}^R(x,0) = \bar{E}^L(x,0) = \frac{1}{2}(\mathcal{K}E)(x,0) = \frac{1}{2}A^2(x) + \mathcal{O}(\varepsilon^2), \quad \forall x \in \Omega, \tag{5.64}$$

for the condition $u_t^\varepsilon(x, 0) = 0$ and

$$\bar{E}^L(x, 0) = 0, \quad \bar{E}^R(x, 0) = (\mathcal{K}E)(x, 0) = A^2(x) + \mathcal{O}(\varepsilon^2), \qquad \forall x \in \Omega, \quad (5.65)$$

for the condition $u_t^\varepsilon(x, 0) = -\frac{i}{\varepsilon} u_0^\varepsilon(x)$. We have Ω-periodic boundary conditions in x for both $\bar{E}^R$ and $\bar{E}^L$. The fluxes $\bar{F}^R$ and $\bar{F}^L$ will be computed from a micro problem based on the expression in Section 5.1.

We need to be careful when discretizing (5.63) in order to capture transmission and reflection of energy around jumps in the material. We must consider the discretized energy E^R and E^L as the *ingoing* energy to the grid point, e.g., E^R is the ingoing from left energy and travels from left to right. Similarly, E^L is the energy that travels from right to left. For the fluxes we argue as follows: The flux F_R^R is the transmitted flux from the left going energy plus the reflected flux from the left going energy. Moreover, F_L^R is the reflected flux from the right going energy plus the transmitted flux from the right going energy. The quantities F_R^L and F_L^L are defined analogously. We illustrate this in Figure 5.1 where we show a numerical example for a jump. The fluxes are sampled for an inbound right ingoing energy $E^R = 1$, with zero ingoing left energy. Note that when a is smooth there will be almost no reflection and only transmitted flux.

Based on this observation we choose to discretize (5.63) with an upwind scheme for the right and left going energy $\bar{E}^R$ and $\bar{E}^L$,

$$\begin{cases} (\bar{E}^R)_m^{n+1} = (\bar{E}^R)_m^n - \lambda \left((\bar{F}_L^R)_m^n - (\bar{F}_R^R)_{m-1}^n \right), \\ (\bar{E}^L)_m^{n+1} = (\bar{E}^L)_m^n - \lambda \left((\bar{F}_L^L)_{m+1}^n - (\bar{F}_R^L)_m^n \right), \end{cases} \qquad \lambda = \frac{\Delta t}{\Delta x}. \quad (5.66)$$

Next we will describe how to compute all the flux quantities in (5.66) above by solving a micro problem with the macroscopic variables $(\bar{E}^R)_m^n$, $(\bar{E}^R)_m^n$, t_n and x_m as input.

Reconstruction Operator and Micro Problem

In this section we describe the micro problem which shall provide the macro scheme with the missing information, the flux. The micro problem will be of the form (5.1) but without boundary conditions. The input to the micro problem are the macroscopic variables x_m, t_n, $(\bar{E}^R)_m^n$ and $(\bar{E}^L)_m^n$. We will use the notation $\mathcal{E}^R := (\bar{E}^R)_m^n$, $\mathcal{E}^L := (\bar{E}^L)_m^n$, for the ingoing energy from right and left respectively; $t' := t_n$; and $x' := x_m$ to make the notation simpler.

We make a change of variables in the micro problem such that $x - x' \mapsto x$ and $t - t' \mapsto t$. This implies that $a(x) \mapsto a(x + x')$. The micro problem is formulated as an initial value problem:

$$\begin{cases} v_{tt}^\varepsilon - \partial_x(a^2 v_x^\varepsilon) = 0, \qquad Y^\varepsilon \times [-\tau, \tau], \\ v^\varepsilon(x, 0) = \sqrt{\mathcal{E}^R} \exp\left(i\alpha(x, 0)/\varepsilon\right) + \sqrt{\mathcal{E}^L} \exp(i\beta(x, 0)/\varepsilon), \\ v_t^\varepsilon(x, 0) = -\frac{i}{\varepsilon} v^\varepsilon(x, 0), \end{cases} \quad (5.67)$$

where α, β are matched with a at $t = 0$,

$$\alpha(x, 0) = -\beta(x, 0) = \int_0^x \frac{\mathrm{d}s}{a(s)}. \tag{5.68}$$

The micro box Y^ε is chosen big enough so that effects from the boundary does not reach inside the domain $[-\eta, \eta]$ for time $-\tau \leq t \leq \tau$. Typically we use $Y^\varepsilon = [-y_{\max}, y_{max}]$ where $y_{\max} = \eta + \tau \max a$. Other techniques for numerically simulating infinite domains are standard absorbing boundary conditions (ABC) [26] and perfectly matched layers (PML) [8, 15].

We shall now give a motivation to why we choose these initial conditions. In the language of HMM the step $\mathcal{E}^R, \mathcal{E}^L \mapsto v^\varepsilon$ is called the reconstruction step. The approximation should be such that v^ε satisfies the wave equation and v^ε has an energy approximately the same as $\mathcal{E}^R + \mathcal{E}^L$.

The asymptotic solution v^ε to (5.67) can be written as a bi-directional wave,

$$v^\varepsilon(x, t) \simeq A_0(x, t) \exp(i\alpha(x, t)/\varepsilon) + B_0(x, t) \exp(i\beta(x, t)/\varepsilon). \tag{5.69}$$

For a one way wave, going right $B_0 = 0$ the local mean (scaled) energy of that solution will then be equal to $A_0^2 + \mathcal{O}(\varepsilon^2)$. Similarly, for a left going one wave, the local mean (scaled) energy will be equal to $B_0^2 + \mathcal{O}(\varepsilon^2)$. We therefore pick $A_0 = \sqrt{\mathcal{E}^R}$ and $B_0 = \sqrt{\mathcal{E}^L}$. The initial condition u_t^ε is chosen to match (5.69). Indeed,

$$v_t^\varepsilon \approx \frac{i}{\varepsilon} A_0 \left(\alpha_t \exp(i\alpha/\varepsilon) + \beta_t B_0 \exp(i\beta/\varepsilon) \right), \tag{5.70}$$

and by (5.5) and (5.69) we have that,

$$v_t^\varepsilon(x, 0) = -\frac{i}{\varepsilon} u^\varepsilon(x, 0). \tag{5.71}$$

We use a Leapfrog finite difference scheme for (5.67). It is based on central differences in both time and space. We use a uniform grid such that $\lambda = \Delta t / \Delta x$ is constant. The scheme reads:

$$\begin{cases} v_m^{n+1} = 2v_m^n - v_m^{n-1} + \dfrac{\Delta t^2}{\Delta x} \left((av_x^\varepsilon)_{m+\frac{1}{2}}^n - (av_x^\varepsilon)_{m-\frac{1}{2}}^n \right), & 0 \leq n < N, \\[2mm] \text{where} \quad (av_x^\varepsilon)_{m\pm\frac{1}{2}}^n = \pm\dfrac{a_{m\pm\frac{1}{2}}}{\Delta x} \left(v_{m\pm1}^n - v_m^n \right). \end{cases} \tag{5.72}$$

Since we are using a two-step method we require a one-step method to initialize the method. We have chosen to set

$$v_m^{-1} = \underbrace{u^\varepsilon(x_m, 0)}_{=v_0^\varepsilon(x)} - \Delta t \underbrace{v_t^\varepsilon(x_m, 0)}_{=v_1^\varepsilon} + \frac{\Delta t^2}{2} \underbrace{v_{tt}^\varepsilon(x_m, 0)}_{=\partial_x(a^2 v_x^\varepsilon)} + \mathcal{O}(\Delta t^3), \tag{5.73}$$

where $\partial_x(a^2 v_x^\varepsilon)$ is discretized as above. See [34] for implementation details.

Remark 19. *Suppose we have a matched phase ϕ such that $\phi_x = 1/a$ and*

$$\phi(x,0) = \phi(x',0) + (x-x')\phi_x(x',0) + \mathcal{O}((x-x')^2). \qquad (5.74)$$

Then it is possible, with little loss of asymptotic accuracy, to use an approximation of the initial data in (5.67) of the form,

$$v^\varepsilon(x,0) \approx \sqrt{\mathcal{E}^R}\exp\left(\frac{i(x-x')}{\varepsilon a(x)}\right) + \sqrt{\mathcal{E}^L}\exp\left(\frac{-i(x-x')}{\varepsilon a(x)}\right). \qquad (5.75)$$

The error in the initial data with respect to the scaled energy $\mathcal{E}^R$ and $\mathcal{E}^L$ will be proportional to ε instead of ε^2.

Compression Operator

Once we have solved (5.67) for u^ε we obtain the macroscopic unknowns $\bar{F}^R$ and $\bar{F}^L$ by computing the local mean in the point (x',t'), which is just $x=0$ and $t=0$ in the local coordinate system,

$$\bar{F}^R \approx -\frac{\varepsilon^2}{4}\mathcal{K}\left(a|u_t^\varepsilon - au_x^\varepsilon|^2\right), \quad \bar{F}^L \approx \frac{\varepsilon^2}{4}\mathcal{K}\left(a|u_t^\varepsilon + au_x^\varepsilon|^2\right). \qquad (5.76)$$

The quantities u_t^ε and u_x^ε are thus needed to compute the fluxes. These are computed from the discrete solution u_m^n at time t_n at x_m with a second order finite difference scheme:

$$\begin{cases} (u_t^\varepsilon)_m^{n+1} = \dfrac{u_m^{n+1} - u_m^{n-1}}{2\Delta t} + \Delta t\,\partial_x(a^2(x_m)u_x^\varepsilon(x_m,t_n)), & 0 \le n < N, \\[2mm] u_x^\varepsilon(x_m,t_n) = \dfrac{u_{m+1}^n - u_{m-1}^n}{2\Delta x}, & 0 \le n \le N, \end{cases} \qquad (5.77)$$

where $\partial_x(a^2(x_m)u_x^\varepsilon(x_m,t_n))$ is discretized in the same way as in the micro solver.

In the case when we have a jump or sharp variations in a we sample two values for both $\bar{F}^R$ and $\bar{F}^L$. One value on each side of the jump for each flux. This will represent the ingoing and reflected energy corresponding to which side the inbound energy comes from. To illustrate the idea we show in Figure 5.1 a micro problem computation from the numerical example found in [25], where we have a jump in a at $x = 0.5$.

Finally, an algorithm summary is found in Algorithm 5.1.

Remark 20. *We note that we can precompute the micro problems by observing that, for $\vec{E} = \begin{bmatrix} \bar{E}^R & \bar{E}^L \end{bmatrix}^T$,*

$$\begin{cases} \bar{F}^R(x_m,\vec{E}) = \bar{E}^R\bar{F}^R(x_m,e_1) + \bar{E}^L\bar{F}^R(x_m,e_2), \\ \bar{F}^L(x_m,\vec{E}) = \bar{E}^R\bar{F}^L(x_m,e_1) + \bar{E}^L\bar{F}^L(x_m,e_2), \end{cases} \qquad (5.78)$$
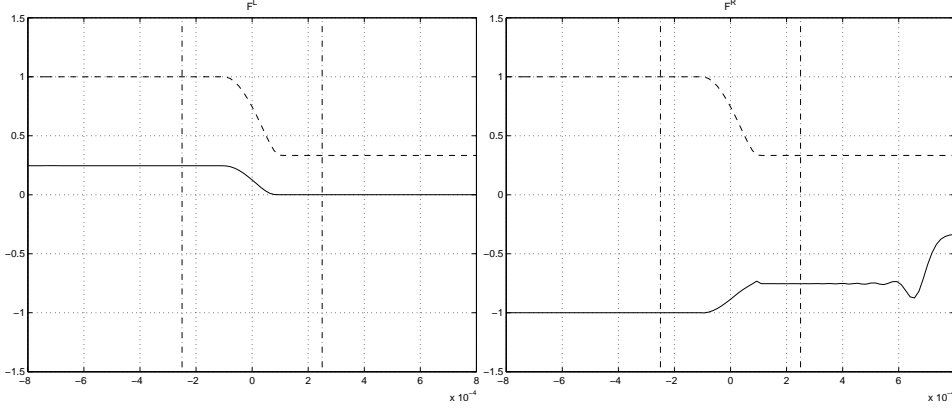
Figure 5.1: The fluxes F^L (left figure) and F^R (right figure) visualized for an incoming wave from the right, $E^R = 1$, $E^L = 0$. The material a (dashed line) shows the jump in the middle of the microbox from $a = 1$ on the left side, down to $a = 1/3$ on the positive right side. The two vertical dashed lines are the sampling points where we compute the right F^R_R and left flux F^R_L. We see in the left figure the reflection at the left side of the jump and in the right picture we see the transmission to the right of the jump.

where

$$e_1^T = \begin{bmatrix} 1 & 0 \end{bmatrix}, \quad e_2^T = \begin{bmatrix} 0 & 1 \end{bmatrix}. \tag{5.79}$$

Thus it is enough to compute the matrices S_m for each grid point x_m,

$$S_m = \begin{bmatrix} \bar{F}^R(x_m, e_1) & \bar{F}^R(x_m, e_2) \\ \bar{F}^L(x_m, e_1) & \bar{F}^L(x_m, e_2) \end{bmatrix}, \qquad 0 \leq m \leq M, \tag{5.80}$$

i.e., solve one micro problem per macro grid point. We then formulate the flux $\bar{F}(x_m, \vec{E})$ for some grid point x_m as a linear mapping via the transfer matrix S_m,

$$\bar{F}(x_m, \vec{E}) = \begin{bmatrix} \bar{F}^R(x_m, \vec{E}) \\ \bar{F}^L(x_m, \vec{E}) \end{bmatrix} = S_m \vec{E} \tag{5.81}$$

Note that for smooth a with $|a_x|$ small, S will be almost diagonal. In the case when a has a jump we sample the flux on two places, to the left and to the right of the jump, thus obtaining two different matrices for that grid-point, $(S^R)_m$ and $(S^L)_m$. One matrix for each side of the the jump. In the case when we cannot say for sure where there is a jump we can choose to always compute both matrices for each grid-point.

Algorithm 5.1 HMM algorithm for the wave equation. Uses microsolver Algorithm 5.2

.

Discretize domain Ω into $x_0, x_1, \ldots, x_m \in \Omega$ and time $[0, T]$ into $t_0, t_1, \ldots, t_N$ such that the grid x_k is aligned with the macro grid, and the initial data is resolved, and $\lambda = \frac{\Delta t}{\Delta x}$ satisfies the CFL condition $a_{\max} \frac{\Delta t}{\Delta x} \leq 1$.

Compute initial data $\bar{E}_m^0$ from $\mathcal{E}^R$ and $\mathcal{E}^L$ as in (5.67).

OPTIONAL: Precompute fluxes:

for $n = 0, 1, \ldots, N$ **do**

   Precompute fluxes as described in Remark. 20.

end for

MAIN LOOP: time step solution:

for $n = 0, 1, \ldots, N$ **do**

   $(\bar{E}^R)_m^{n+1} = (\bar{E}^R)_m^n - \lambda \left((\bar{F}_L^R)_m^n - (\bar{F}_R^R)_{m-1}^n \right)$

   $(\bar{E}^L)_m^{n+1} = (\bar{E}^L)_m^n - \lambda \left((\bar{F}_L^L)_{m+1}^n - (\bar{F}_R^L)_m^n \right)$

end for

Algorithm 5.2 microsolver: Compute $\tilde{F}$ given $x', \mathcal{E}^R$ and $\mathcal{E}^L$.

Pick Y^ε such that $Y^\varepsilon = [-y_{\max}, y_{\max}]$ and $y_{\max} = \eta + \tau \max_{x \in Y^\varepsilon} a(x)$.

Discretize Y^ε into $x_0, x_1, \ldots, x_M$ and time $[-\tau, \tau]$ into $t_0, t_1, \ldots, t_N$ such that $\frac{\varepsilon}{\Delta x} = \rho$ (points per wave length measure) and $\lambda = \frac{\Delta t}{\Delta x}$ satisfies the CFL condition $a_{\max} \frac{\Delta t}{\Delta x} \leq 1$.

Compute initial data $(v^\varepsilon)_m^0 = \ldots$ and $(v^\varepsilon)_m^{-1} = \ldots$.

for $n = 0, 1, \ldots, n$ **do**

   Compute $(u^\varepsilon)_m^{n+1}$ according to (5.72).

   Compute auxiliary variables $(u_t^\varepsilon)_m^n$ and $(u_x^\varepsilon)_m^n$ as in (5.77).

   Compute $(G^R)^n$ as $-\frac{\varepsilon^2}{4} \int K_\eta a |v_t^\varepsilon - a v_x^\varepsilon|$ on

   Compute $(G^L)^n$ as $\frac{\varepsilon^2}{4} \int K_\eta a |v_t^\varepsilon + a v_x^\varepsilon|$ on

end for

Compute $F^R = (\mathcal{K}_\tau G^R)(\xi, \varphi)$.

IMPORTANT: If this macro grid point has a jump of width δ we use, instead of a kernel and a point sampling at $x = \pm\delta$ and at $t = \tau$.

5.3 Numerical Results

In this experiment we will consider a wave traveling through a constant medium with $a_0 = 1$ to the left of $b_0 = 0.45$ and to the right of $b_1 = 0.55$. In between $b_0 \le x \le b_1$ we have $a_1 = 1/3$. The material has a smooth jump from $a_0 \leftrightarrow a_1$ at the points b_0 and b_1. The width of the jumps is denoted δ. We have constructed $a(x)$ as the square root of $a^2(x)$ where a^2 is continuously differentiable for all $0 \le x \le 1$. The form of $a^2(x)$ is,

$$a^2(x) = \begin{cases} a_0^2 & 0 \le x < -\frac{\delta}{2} + b_0, \\ a_0^2 + (a_1^2 - a_0^2)v\left(\frac{(x-b_0)+\frac{\delta}{2}}{\delta}\right) & -\frac{\delta}{2} + b_0 \le x \le \frac{\delta}{2} + b_0, \\ a_1^2 & \frac{\delta}{2} + b_0 < x < -\frac{\delta}{2} + b_1 < x < \frac{\delta}{2} + b_1 \\ a_1^2 + (a_0^2 - a_1^2)v\left(\frac{(x-b_1)+\frac{\delta}{2}}{\delta}\right) & -\frac{\delta}{2} + b_1 \le x \le \frac{\delta}{2} + b_1, \\ a_0^2 & \frac{\delta}{2} + b_1 < x \le 1, \end{cases}$$

where

$$\begin{cases} a_0 = 1, \quad a_1 = \dfrac{1}{3}, \\ b_0 = 0.45, \quad b_1 = 0.55, \\ \delta = 0.0005, \quad v(x) = -2x^3 + 3x^2. \end{cases} \tag{5.82}$$

Note that a^2 is made 1-periodic outside $\Omega = [0, 1]$ in some suitable way. We show a graph of a in Figure 5.6.

From theory we know that in the limit as $\delta \to 0$ the amplitude of the reflected wave $u_{\text{ref}}^\varepsilon$ will be of order $\gamma |u_{\text{inc}}^\varepsilon|$ where $u_{\text{inc}}^\varepsilon$ is the incident wave that hits the discontinuity from the left and γ is the reflection coefficient given by [33],

$$\gamma = \frac{a_0 - a_1}{a_0 + a_1}.$$

In the limit of our setup we have $\gamma = 0.5$, i.e., the reflected wave will be half the amplitude of the incident wave.

The interesting part in this experiment is that geometrical optics (GO) fails to capture this reflection effect. The coarse scale GO solution will travel through the jump unaffected.

At the jump $x_m = 0.45$ or $x_m = 0.55$ we use 128 grid points per ε in the micro problem to accurately capture the effects of the jump. For all other macro grid points we use the analytical form that $F^R = aE$ and $F^L = -aE$ to compute the fluxes. For the micro problem we used $\varepsilon = 0.5 \cdot 10^{-3}$, $\eta = \varepsilon$, $\tau = 2\varepsilon$, $\lambda \approx 1$. In this example we did not use a kernel, instead we point sampled the fluxes at a fixed $x = \pm\eta/4$ with respect to the center of the micro box (seen in Figure 5.1).

The transmission matrices S^R and S^L at the jump at $x = 0.45$ are,

$$S^R = \begin{bmatrix} -0.75382 & -0.082062 \\ 0 & 0.33333 \end{bmatrix}, \quad S^L = \begin{bmatrix} -1 & 0 \\ 0.24619 & 0.25127 \end{bmatrix}, \tag{5.83}$$
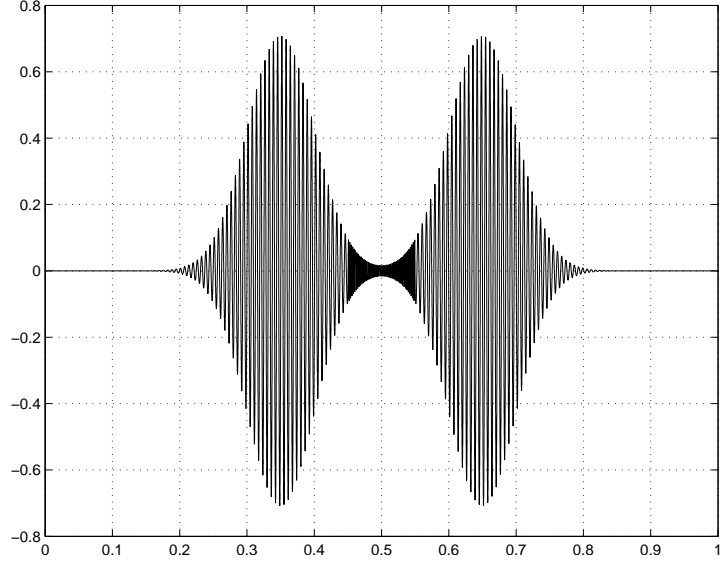
Figure 5.2: The initial wave u^ε (real part) for numerical experiment 5.3.

and at the jump at $x = 0.55$ they are,

$$S^R = \begin{bmatrix} -0.25127 & -0.24619 \\ 0 & 1 \end{bmatrix}, \quad S^L = \begin{bmatrix} -0.33333 & 0 \\ 0.082062 & 0.75382 \end{bmatrix}. \tag{5.84}$$

We present the initial data and the numerical results at $t = 0$ and at $t = T$ in Figure 5.2, 5.3, 5.4 and 5.5. We see that our numerical method accurately captures the reflected energy on both left and right side of the middle obstacle which lower wave propagation speed.
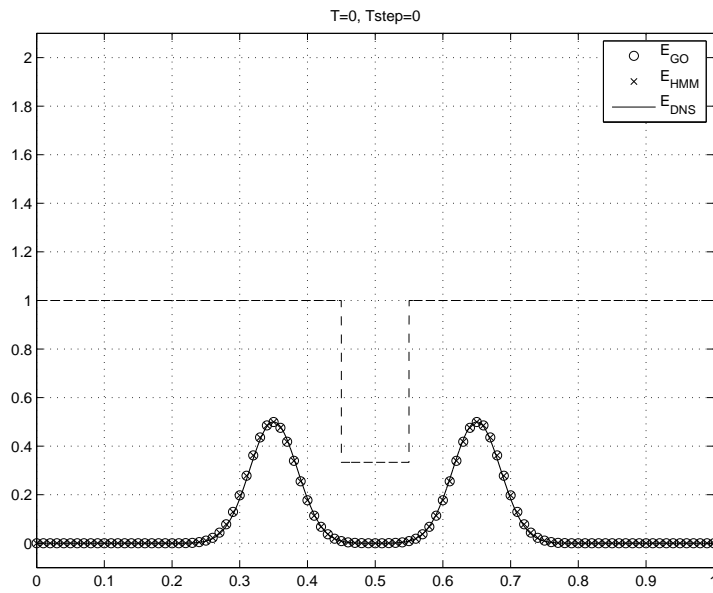
Figure 5.3: Initial energy at $t = 0$ for numerical experiment 5.3. The energy on the left side of the jump is right going, and the energy on the right side of the jump is left going.
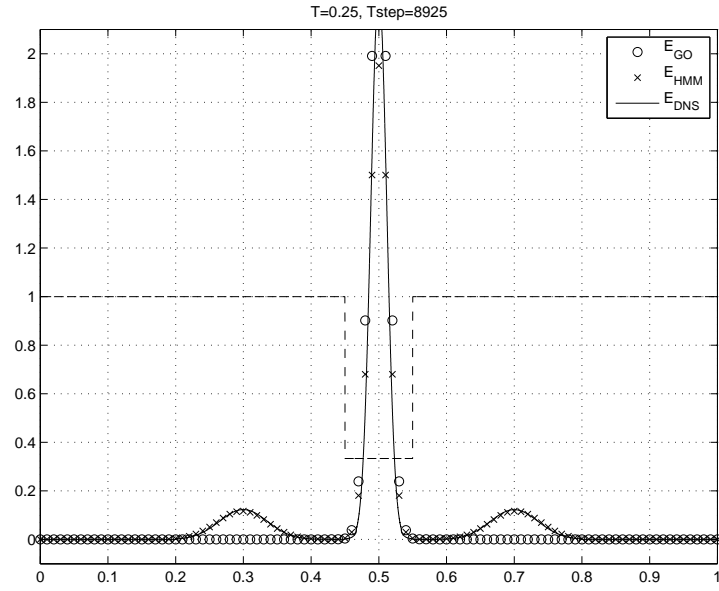
Figure 5.4: Energy $\bar{E}$ at $t = T$ for the numerical experiment 5.3. On each side of the jump we see the energy that was reflected from the jump.
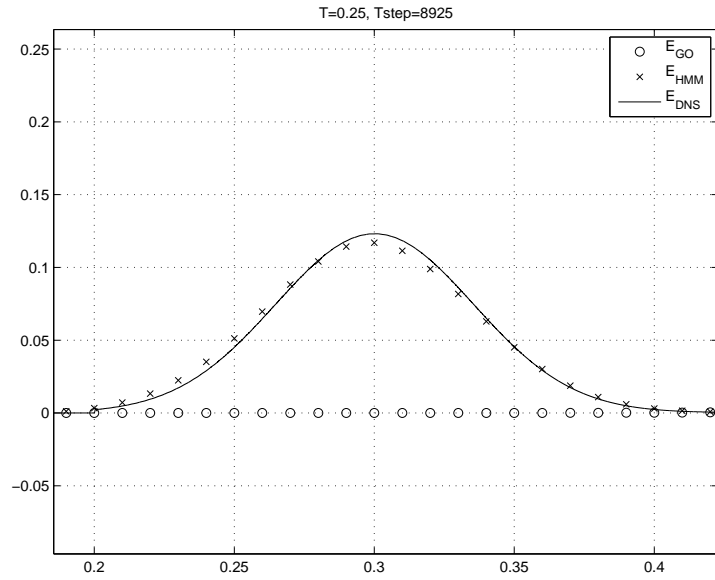

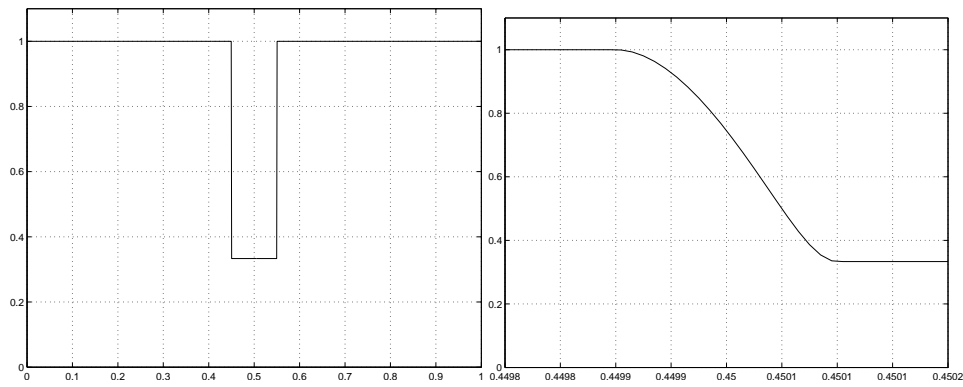Figure 5.5: Energy $\bar{E}$ at $t = T$ for the numerical experiment 5.3 zoomed at left reflection.

Figure 5.6: The material used in the numerical experiment 5.3: $a(x)$ plotted over $0 \leq x \leq 1$ with a jump $a = a_0$ to $a = a_1$ at $x = b_0$ and another jump from $a = a_1$ to $a = a_0$ at $x = b_1$.

Chapter 6

Future Work

In this chapter we discuss ideas that can be added to the work we have done on the subject of numerical methods for multiscale wave propagation.

6.1 Long Time Wave Propagation with Well-Posed Macroscopic PDE

One issue related to our proposed HMM method for long time wave propagation, e.g., where $T^\varepsilon = \mathcal{O}(\varepsilon^{-2})$, is that it is based on an ill-posed model equation,

$$u_{tt} - \partial_x F = 0, \quad F = \bar{A}u_x + \beta\varepsilon^2 u_{xxx}, \qquad \Omega \times [0, T^\varepsilon].$$

Even though the initial data is band limited, local truncation errors accumulate and the numerical solution blows up. As we described in Section 2.5, the equation needs to be regularized to be of any practical use. This raises a question of the methods usability. For instance, in an engineering application it could prove difficult to accurately determine correct choice of regularization. We have used a low-pass filtering technique based on coarse grids and we speculate that determining the correct grid size could be difficult in a real world application. To address this problem, and as future work on HMM for long time wave propagation problems, it would be interesting to try and use another method for the reconstruction of the micro problem, using u_x and u_{xtt} instead of u_x and u_{xxx}. This approach would be consistent with the well-posed equation in Remark 18,

$$u_{tt} - \partial_x F = 0, \quad F = \bar{A}u_x + \varepsilon^2 \frac{\beta}{\bar{A}} u_{xtt} = 0, \qquad \Omega \times [0, T^\varepsilon].$$

6.2 High Contrast Problem

Wave propagation in periodic elastic composites with high contrast has been studied by Smyshlyaev [50] in the context of non-classical homogenization of so called high

contrast problems [12, 5, 51]. The setting is the following. We assume that $A^\varepsilon(x) = A(x, x/\varepsilon)$ where $A(x, y)$ is 1-periodic in $y \in Y = [0, 1]^d$. Furthermore, assume that $A(x, y) = \delta$ in a "porous cavity" in Y. Outside the cavity A is assumed to be positive and independent of δ and ε. Smyshlyaev showed that in the limit as $\varepsilon \to 0$ and where the porosity is of so called "double porosity type" [4], e.g., $\delta = \varepsilon^2$, the micro and macro scales are coupled in a non-trivial way. The effective equation in this case will be two coupled wave equations. One equation over the macroscopic domain Ω and one equation over a periodic cell Y.

6.3   Bloch Waves

So far we have only considered solutions of the wave equation where the material A^ε has fast variations of the order ε and the initial data is slowly varying; or the material is smooth but the initial data is highly oscillatory. Another interesting regime is when the variations in A^ε is of the same order as the oscillations in the initial data. The effective equation in this case will be the amplitude v, which solves a non-oscillatory wave equation and is related to the oscillatory solution $u^\varepsilon(x, t)$ by,

$$u^\varepsilon(x, t) = v(x, t) \exp(i\omega t/\varepsilon)\Psi(x/\varepsilon),$$

where Ψ and ω are the Bloch function with its corresponding eigenvalue. One important application related to this regime is the numerical simulation of meta materials. Meta materials are artificial materials which gain their properties from structure rather than composition, using small inhomogeneities to create effective macroscopic behavior [20]. A big motivation behind the research on meta materials are the "negative index of reflection" materials (NIM).

6.4   HMM for High Frequency Wave Propagation in Higher Dimensions

In [23] we demonstrated an HMM method for high frequency wave propagation problems in one dimension. The main new difficulty in higher dimensions, is the fact that the solution in general is made up of any number of waves going in any directions, not just two waves going backwards and forwards as in one dimension.

One way to treat this case is to explicitly keep track of the directions of the waves and solve them individually. Each wave would have its own amplitude and phase. These would be the macroscopic variables. The direction would correspond to the gradient of the phase. To update the amplitudes and phases from the solution of a micro problem one would need some filtering mechanism. The issue of how to add new waves, which appear for instance at caustics, must also be addressed.

Another way to approach the multi-dimensional case would be to consider the energy as a function of angle $E = E(x, t, \theta)$, representing the wave energy propagating in the θ-direction, in analogue with the E^L and E^R energies for the one-dimensional case. In the high frequency limit this energy function satisfies the

Liouville equation

$$E_t + v(x, \theta) \cdot \nabla_x E + d(x, \theta) E_\theta = 0,$$

where

$$v(x, \theta) = a(x)(\cos \theta, \sin \theta), \qquad d(x, \theta) = \nabla a(x) \cdot (\sin \theta, -\cos \theta).$$

The macroscopic equation would hence be set in one dimension higher than the wave equation, but it would be independent of ε. In an HMM method E would be discretized also in θ. The micro problems would still solve the wave equation.

Bibliography

[1] Assyr Abdulle and Weinan E. Finite difference heterogeneous multi-scale method for homogenization problems. *J. Comput. Phys.*, 191(1):18–39, 2003.

[2] Assyr Abdulle and Marcus J. Grote. Finite element heterogeneous multiscale method for the wave equation. *Multiscale Modeling & Simulation*, 9(2):766–792, 2011.

[3] A. Allaire, A. Braides, G. Buttazzo, A. Defranceschi, and L. Gibiansky. School on homogenization. *SISSA Ref. 140/73/M*, 1993.

[4] Todd Arbogast, Jim Douglas, Jr., and Ulrich Hornung. Derivation of the double porosity model of single phase flow via homogenization theory. *SIAM J. Math. Anal.*, 21:823–836, May 1990. ISSN 0036-1410.

[5] NO Babych, IV Kamotski, and Valery P Smyshlyaev. Homogenization of spectral problems in bounded domains with doubly high contrasts. *Netw. Heterogen. Media*, 3:413–436, 2008.

[6] Jean-David Benamou. Big ray tracing: Multivalued travel time field computation using viscosity solutions of the eikonal equation. *Journal of Computational Physics*, 128(2):463–474, 1996.

[7] Alain Bensoussan, Jacques-Louis Lions, and George Papanicolaou. *Asymptotic Analysis in Periodic Structures*. North-Holland Pub. Co., 1978. ISBN 0444851720.

[8] Jean-Pierre Berenger. A perfectly matched layer for the absorption of electromagnetic waves. *Journal of Computational Physics*, 114(2):185 – 200, 1994. ISSN 0021-9991.

[9] M. Born, E. Wolf, and A.B. Bhatia. *Principles of optics: electromagnetic theory of propagation, interference and diffraction of light.* Cambridge University Press, 1999. ISBN 9780521642224.

[10] Susanne C. Brenner and L. Ridgway Scott. *The Mathematical Theory of Finite Element Methods.* Springer, 2nd edition, April 2002. ISBN 0387954511.

[11] J. W. Brown and R. V. Churchill. *Fourier Series and Boundary Value Problems.* McGraw-Hill Publishing Co., 2001.

[12] KD Cherednichenko, Valery P Smyshlyaev, and VV Zhikov. Non-local homogenized limits for composite media with highly anisotropic periodic fibres. *Proceedings of the Royal Society of Edinburgh: Section A Mathematics*, 136 (01):87–114, 2006.

[13] Doina Cioranescu and Patrizia Donato. *An Introduction to Homogenization.* Number 17 in Oxford Lecture Series in Mathematics and its Applications. Oxford University Press Inc., 1999.

[14] B. Cockburn, G. Karniadakis, and C.W. Shu. *Discontinuous Galerkin Methods, Theorie, Computation and Applications.* Springer, 2000.

[15] Kenneth Duru. *Perfectly Matched Layers for Second Order Wave Equations.* Licentiate thesis, Department of Information Technology, Uppsala University, May 2010.

[16] Weinan E and Björn Engquist. The heterogeneous multiscale methods. *Commun. Math. Sci.*, pages 87–133, 2003.

[17] Weinan E, Björn Engquist, and Zhongy Huang. Heterogeneous multiscale method: A general methodology for multiscale modeling. *Phys. Rev. B: Condens. Matter Mater. Phys.*, 67(9):092101, Mar 2003.

[18] Weinan E, Björn Engquist, Xiantao Li, Weiqing Ren, and Eric Vanden-Eijnden. Heterogeneous multiscale methods: A review. *Commun. Comput. Phys.*, 2(3):367–450, 2007.

[19] Weinan E, Pingbing Ming, and Pingwen Zhang. Analysis of the heterogeneous multiscale method for elliptic homogenization problems. *J. Amer. Math. Soc.*, 18(1):121–156, 2004.

[20] N. Engheta, R.W. Ziolkowski, Institute of Electrical, and Electronics Engineers. *Metamaterials: physics and engineering explorations.* Wiley-Interscience, 2006. ISBN 9780471761020.

[21] Björn Engquist, Henrik Holst, and Olof Runborg. Multiscale methods for the wave equation. In *Sixth International Congress on Industrial Applied Mathematics (ICIAM07) and GAMM Annual Meeting*, volume 7. Wiley, 2007.

[22] Björn Engquist, Henrik Holst, and Olof Runborg. Analysis of HMM for one dimensional wave propagation problems over long time. *arXiv:1111.2541v1*, 2011.

[23] Björn Engquist, Henrik Holst, and Olof Runborg. Multiscale methods for one dimensional wave propagation with high frequency initial data. Technical report, School of Computer Science and Communication, KTH, 2011. TRITA-NA 2011:7.

[24] Björn Engquist, Henrik Holst, and Olof Runborg. Multiscale methods for the wave equation. *Comm. Math. Sci.*, 9(1):33–56, Mar 2011.

[25] Björn Engquist, Henrik Holst, and Olof Runborg. Multiscale methods for wave propagation in heterogeneous media over long time. In Björn Engquist, Olof Runborg, and Richard Tsai, editors, *Numerical Analysis and Multiscale Computations*, volume 82 of *Lect. Notes Comput. Sci. Eng.*, pages 167–186. Springer Verlag, 2011.

[26] Björn Engquist and Andrew Majda. Absorbing Boundary Conditions for the Numerical Simulation of Waves. *Mathematics of Computation*, 31(139):629–651, 1977. ISSN 00255718.

[27] Björn Engquist and Olof Runborg. Multiphase computations in geometrical optics. *J. Comp. Appl. Math*, 74:175–192, 1996.

[28] Björn Engquist and Olof Runborg. Computational high frequency wave propagation. *Acta Numer.*, 12:181–266, 2003.

[29] Björn Engquist, Olof Runborg, and Anna-Karin Tornberg. High frequency wave propagation by the segment projection method. *J. Comp. Phys*, 178:373–390, 2002.

[30] Björn Engquist and Panagiotis E. Souganidis. Asymptotic and numerical homogenization. *Acta Numer.*, 17:147–190, 2008.

[31] Björn Engquist and Yen-Hsi Tsai. Heterogeneous multiscale methods for stiff ordinary differential equations. *Math. Comp.*, 74(252):1707–1742, 2005.

[32] B. Gustafsson, H. O. Kreiss, and J. Oliger. *Time Dependent Problems and Difference Methods*. Wiley, New York, 1995.

[33] Eugene Hecht. *Optics (4th Ed.)*. Addison Wesley, 2001.

[34] Henrik Holst. Algorithms and codes for wave propagation problems. Technical report, CSC/NA, 2011. TRITA-NA 2011:6.

[35] V. V. Jikov, S. M. Kozlov, and O. A. Oleinik. *Homogenization of Differential Operators and Integral Functions*. Springer, 1991.

[36] Joseph B. Keller. Geometrical theory of diffraction. *J. Opt. Soc. Am.*, 52(2):116–130, Feb 1962.

[37] I. G. Kevrekidis, C. W. Gear, J. Hyman, P. G. Kevekidis, and O. Runborg. Equation-free, coarse-grained multiscale computation: Enabling microscopic simulators to perform system-level tasks. *Comm. Math. Sci.*, pages 715–762, 2003.

[38] Agnes Lamacz. Dispersive effective models for waves in heterogeneous media. *Math. Models Methods Appl. Sci.*, 21:1871–1899, 2011.

[39] R.J. LeVeque. *Numerical Methods for Conservation Laws.* Lecture Notes in Mathematics. Birkhäuser Verlag AG, 1994. ISBN 9783764327231.

[40] X. Li and W. E. Multiscale modelling of the dynamics of solids at finite temperature. *J. Mech. Phys. Solids*, 53:1650–1685, 2005.

[41] V. A. Marchenko and E. Y. Khruslov. Homogenization of partial differential equations. *Progress in Mathematical Physics*, 46, 2006.

[42] O. Marin, O. Runborg, and A.-K. Tornberg. Corrected trapezoidal rules for a class of singular functions. submitted BIT, 2011.

[43] Gianni Dal Maso. *Introduction to Γ-Convergence, An.* Birkhüser Boston, 1993. ISBN 081763679X.

[44] Ana-Maria Matache and Christoph Schwab. Generalized p-FEM in homogenization. *Appl. Numer. Math.*, 33, 2000.

[45] Pingbing Ming and Xingye Yuen. Numerical methods for multiscale elliptic problems. *J. Comput. Phys.*, 214(1):421–445, 2005.

[46] Gabriel Nguetseng. A general convergence result for a functional related to the theory of homogenization. *SIAM J. Math. Anal.*, 20(3):608–623, 1989. ISSN 0036-1410.

[47] Grigorios A. Pavliotis and Andrew M. Stuart. *Multiscale Methods: Averaging and Homogenization.* Springer, 2007.

[48] Giovanni Samaey. *Patch Dynamics: Macroscopic Simulation of Multiscale Systems.* PhD thesis, Katholieke Universiteit Leuven, 2006.

[49] Fadil Santosa and William W. Symes. A dispersive effective medium for wave propagation in periodic composites. *SIAM J. Appl. Math.*, 51(4):984–1005, 1991. ISSN 0036-1399.

[50] Valery P Smyshlyaev. Propagation and localization of elastic waves in highly anisotropic periodic composites via two-scale homogenization. *Mechanics of Materials*, 41(4):434–447, Apr 2009.

[51] Valery P Smyshlyaev and KD Cherednichenko. On rigorous derivation of strain gradient effects in the overall behaviour of periodic heterogeneous media* 1. *Journal of the Mechanics and Physics of Solids*, 48(6-7):1325–1357, 2000.

[52] John C. Strikwerda. *Finite Difference Schemes and Partial Differential Equations (2nd ed.)*. SIAM, 2004. ISBN 0898715679.

[53] Nick M. Tanushev Tanushev, Richard Tsai, and Björn Engquist. A coupled finite difference - gaussian beam method for high frequency wave propagation. *UCLA CAM Reports (submitted)*, pages 10–40, 2010.

[54] Lloyd N. Trefethen. *Spectral methods in MatLab*. Society for Industrial and Applied Mathematics, Philadelphia, PA, USA, 2000. ISBN 0-89871-465-6.

Part II

Included Papers